Lagrangian Computation of Inviscid Compressible Flows

G. H. Klopfer

(NASA-TM-78456) LAGRANGIAN COMPUTATION OF INVISCID COMPRESSIBLE FLOWS (NASA) 60 p HC A04/MF A01 CSCL 12A

N78-24860

Unclas
G3/64 16814

MAY 1978

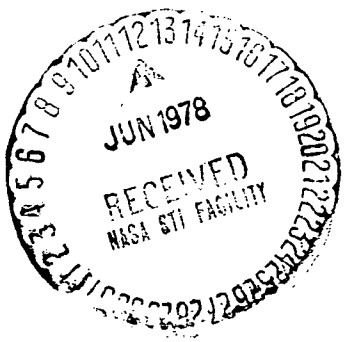

National Aeronautics and
Space Administration

LAGRANGIAN COMPUTATION OF INVISCID COMPRESSIBLE FLOWS

NASA AMES RESEARCH CENTER
MOFFETT FIELD, CA

MAY 78

NASA Technical Memorandum 78456

Lagrangian Computation of Inviscid Compressible Flows

G. H. Klopfer, Ames Research Center, Moffett Field, California

National Aeronautics and
Space Administration

Ames Research Center
Moffett Field, California 94035

LAGRANGIAN COMPUTATION OF INVISCID COMPRESSIBLE FLOWS

G. H. Klopfer*

Ames Research Center

SUMMARY

A Lagrangian method is developed to solve the Euler equations of gas dynamics. The solution of the equations is obtained by a numerical computation with the well-known Flux-Corrected-Transport (FCT) numerical method. This procedure is modified so that the boundary treatment is accurate and relatively simple. Shock waves and other flow discontinuities are captured monotonically without any type of fitting procedures. The Lagrangian method is employed so that the problem of mesh generation is completely avoided. The method is applicable to all Mach numbers except the low subsonic range where compressibility effects are small. The method is applied to a one-dimensional Riemann problem (shock tube) and to a two-dimensional supersonic channel flow with reflecting shock waves.

I. INTRODUCTION

One of the outstanding problems in numerical, transonic-flow calculations is the exact treatment of boundary conditions. Dramatic changes in the transonic flow field are caused by small changes in the boundaries, thus exact computation of the boundary conditions is mandatory. For example, a 1% change in the thickness ratio of an airfoil can change the total lift coefficient more than 10%. Such a strong influence is also seen in the effect a body has on the flow over the airfoil in a three-dimensional wing-body configuration. Furthermore, the curvature at the leading edge of a transonic airfoil has a strong influence on the downstream flow field. Thus, accurate drag polars, for example, are difficult to compute efficiently by present numerical methods.

The current workhorse for numerical computation of inviscid transonic flows is the small-disturbance theory (ref. 1). It can handle steady, unsteady, inviscid, and three-dimensional transonic flows. The boundary conditions are easily satisfied by the small-disturbance theory, but not all types of aerodynamic configurations or flow situations are properly computed within the small-disturbance assumptions. The strong feature of the theory is the simplified treatment of the boundary conditions. The boundary conditions (airfoil slopes) are applied on some mean-surface slit instead of the actual airfoil surface. Multielement and wing-fuselage configurations are

---

*NRC, Resident Research Associate.

thus easily handled. The main drawback of the small disturbance theory is that it is not valid at the wing leading edge, especially wings with blunt leading edges, such as the shock-free peaky airfoils (ref. 2), and for wings at high angles of attack. Another disadvantage is that the small-disturbance shock jump conditions no longer satisfy the Rankine-Hugoniot relations for Mach numbers greater than 1.3.

A more exact approach is to use the full potential equation of transonic flow. These include the method of Jameson (ref. 3) and the hodograph method of Boerstoel (ref. 2). While both methods can treat the boundary condition accurately, they are not straightforward and simple. The Jameson two-dimensional procedure requires that the exterior flow field be mapped numerically into the interior of a circle. The hodograph method is limited to two-dimensional flows, with presently little hope for extension to three dimensions. Of course the potential equation has the same limitation as the small-disturbance equation in that the flows are limited to isentropic flows. Thus no shock Mach numbers greater than 1.3 are allowed.

The Mach number limitation can be overcome by using the full Euler equations. This approach is taken by the finite volume method (ref. 4), the body coordinate transformation (ref. 5), and the Euler-Lagrange method (ref. 6). The most promising seem to be the methods of Rizzi and Thompson. However, the body coordinate method of Thompson is rather complicated and numerically inefficient, especially in the case of an oscillating flap-airfoil configuration. The Euler-Lagrange methods of the Los Alamos group (ref. 6) are rather disappointing for transonic flows in that the shock waves are not captured very well and their schemes require large computational effort. The good feature about all the above approaches is that the boundary conditions can be included to the same order of accuracy as the numerical schemes employed.

Rather than try to improve any of the above methods, we have chosen a different approach altogether. It is a purely Lagrangian approach, unlike the methods of Harlow and Amsden, which still use the physical coordinates as the independent variables. In the purely Lagrangian approach the independent variables are the Lagrangian coordinates (ref. 7). To obtain the Lagrangian equations of gasdynamics for inviscid, adiabatic and ideal gases, the two-dimensional (say) Euler equations of gasdynamics are transformed into the Lagrangian divergent free form. To the resulting set of equations expressing conservation of mass, momentum, and energy, are added the two kinematic relations defining the location (x,y) of a fluid element identified by the Lagrangian coordinates (a,b). The numerical computation is carried out in the Lagrangian plane.

The salient feature of this approach is that the physical plane is automatically transformed into a rectangular computation plane. No explicit transformation computation as in Thompson's method is required. Another feature is that the initial distribution of fluid elements or particles is completely arbitrary. Thus more particles can be clustered close to the aerodynamic configuration for better resolution. The secular mesh distortion which usually destroys the accuracy of the Lagrangian calculation does not

occur for transonic flows without shear except at stagnation points. All these points will be discussed in section II along with the derivation of the governing equations in terms of an arbitrarily moving mesh system given in Appendix A.

The main disadvantage of Lagrangian methods are the lack of good numerical solution techniques applicable to them. Most of the present "standard" numerical methods were developed for Eulerian systems and do not necessarily work well for Lagrangian systems. Much experimentation with different types of numerical methods was required to arrive at the best method. The results of this experimentation are given in section III.

Several sample problems solved by the present approach are presented in section IV. These include a one-dimensional Riemann problem (bursting diaphragm) and the ordinary oblique shock wave reflection off a channel wall for a two-dimensional case.

In the following sections, we restrict ourselves to one or two dimensions. However, extending the Lagrangian approach to three dimensions is simple and adds no extra complexity other than an extra independent variable. The three-dimensional Lagrangian equations are given in Appendix B.

II. FORMULATION

Governing Equations

The equations of gasdynamics in two dimensions for an arbitrarily moving coordinate system are in conservative form (see appendix A for the derivation).

$$\vec{U}_t + \vec{F}_a + \vec{G}_b + \vec{H} = 0 \qquad (1)$$

with

$$\vec{U} = \begin{bmatrix} J\rho \\ J\rho u \\ J\rho v \\ J\rho E \\ x_a \\ x_b \\ y_a \\ y_b \\ x \\ y \end{bmatrix} ; \quad \vec{F} = \begin{bmatrix} \rho\{y_b(u-u_m) - x_b(v-v_m)\} \\ \rho u\{\quad " \quad\} + y_b p \\ \rho v\{\quad " \quad\} - x_b p \\ \rho E\{\quad " \quad\} + p\{y_b u - x_b v\} \\ -u_m \\ 0 \\ -v_m \\ 0 \\ 0 \\ 0 \end{bmatrix}$$

$$\vec{G} = \begin{bmatrix} \rho\{-y_a(u - u_m) + x_a(v - v_m)\} \\ \rho u\{ \quad " \quad \} - y_a p \\ \rho v\{ \quad " \quad \} + x_a p \\ \rho E\{ \quad " \quad \} + p(-y_a u + x_a v) \\ 0 \\ -u_m \\ 0 \\ 0v_m \\ 0 \\ 0 \\ 0 \end{bmatrix}; \quad \vec{H} = \begin{bmatrix} 0 \\ 0 \\ 0 \\ 0 \\ 0 \\ 0 \\ 0 \\ 0 \\ 0 \\ -u_m \\ -v_m \end{bmatrix}$$

where

u,v Cartesian components (x,y) of the fluid velocity

u_m, v_m Cartesian components (x,y) of the moving mesh

a,b coordinates of the moving coordinate system

x,y coordinates of the fixed Cartesian coordinate system

J $= (x_a\, y_b - x_b\, y_a)$, the Jacobian of the transformation from the moving coordinate system (a,b) to the fixed coordinate system (x,y)

ρ, p density, pressure

$$E = \frac{p}{(\gamma - 1)\rho} + \frac{u^2 + v^2}{2} \quad \text{(polytropic ideal gas)}$$

The four equations for x_a, x_b, y_a, and y_b are obtained by differentiating the last two equations. They are added to keep the system strongly conservative. The first eight equations are sufficient to obtain the velocity, density, and pressure field; the last two are required only to locate the position of the moving coordinates.

The fluid velocity components resolved in the moving coordinate system (a,b) are given by

$$\left.\begin{aligned} u^M &= \frac{y_b}{J} u - \frac{x_b}{J} v \\ v^M &= -\frac{y_a}{J} u + \frac{x_a}{J} v \end{aligned}\right\} \tag{2}$$

The Jacobian matrices of system (1) are given by $\partial\vec{F}/\partial\vec{U}$ and $\partial\vec{G}/\partial\vec{U}$, and the system can be rewritten as

$$\vec{U}_t + A\vec{U}_a + B\vec{U}_b + \vec{H} = 0 \tag{3}$$

with

$$A = \frac{\partial \vec{F}}{\partial \vec{U}} \; ; \; B = \frac{\partial \vec{G}}{\partial \vec{U}}$$

The eigenvalues of A are

$$\lambda_{1,2,3,4} = \left(u^M - u_m^M\right), \left(u^M - u_m^M\right), \left(u^M - u_m^M \pm \frac{c}{J}\sqrt{x_b^2 + y_b^2}\right)$$

$$\lambda_{5,\ldots,10} = 0$$

and those of B are

$$b_{1,2,3,4} = \left(v^M - v_m^M\right), \left(v^M - v_m^M\right), \left(v^M - v_m^M \pm \frac{c}{J}\sqrt{x_a^2 + y_a^2}\right)$$

$$b_{5,\ldots,10} = 0$$

where $c^2 = \gamma p/\rho$ and γ = ratio of the specific heats.

The system of equation (1) is the most general set of equations describing two-dimensional, inviscid, ideal gasdynamics in any arbitrarily moving coordinate system (a,b). The equation describing the conservation of mass, momentum, and energy may be written as

$$\frac{\partial \vec{U}}{\partial t} + \frac{\partial}{\partial a}\left[\vec{U}\left(u^M - u_m^M\right)\right] + \frac{\partial}{\partial b}\left[\vec{U}\left(v^M - v_m^M\right)\right] + \vec{S} = 0 \qquad (4)$$

with

$$\vec{U} = \begin{bmatrix} pJ \\ pJu \\ pJv \\ pJE \end{bmatrix} \; ; \quad \vec{S} = \begin{bmatrix} 0 \\ \frac{\partial}{\partial a}\left(y_b p\right) - \frac{\partial}{\partial b}\left(y_a p\right) \\ -\frac{\partial}{\partial a}\left(x_b p\right) + \frac{\partial}{\partial b}\left(x_a p\right) \\ \frac{\partial}{\partial a}\left(pJu^M\right) + \frac{\partial}{\partial b}\left(pJv^M\right) \end{bmatrix}$$

where superscript M is defined by equation (2). The conserved quantities are $\vec{U}$; $(u^M - u_m^M)$ and $(v^M - v_m^M)$ are the (a,b) components of the relative convection velocity; and $\vec{S}$ are the source terms. The eigenvalues of the Jacobian matrices of equations (4) are

$$\lambda = \left(u^M - u_m^M\right), \left(u^M - u_m^M \pm \frac{c}{J}\sqrt{x_b^2 + y_b^2}\right), \left(u^M - u_m^M\right)$$

$$\beta = \left(v^M - v_m^M\right), \left(v^M - v_m^M \pm \frac{c}{J}\sqrt{x_a^2 + y_a^2}\right), \left(v^M - v_m^M\right)$$

It is interesting to note that the eigenvalues depend strictly on the convective speed and the relative velocities between the convective speed and the sonic speed times some cell distortion factor. This fact remains true for any arbitrarily moving coordinate system. Initially the two coordinate systems can coincide so that $x = a$ and $y = b$, but this is not required. The equations may now be specialized by specifying the mesh velocity.

Eulerian system.- The Eulerian system is characterized by a stationary mesh. Setting $u_m^M = 0$ and $v_m^M = 0$ obtains $x = a$, $y = b$ for all time, thus $x_a = 1$, $y_b = 1$, $x_b = 0$, $y_a = 0$, and $J = 1$. Substituting into equations (1) and (2) obtains ($u^M = u$, $v^M = v$)

$$\left.\begin{aligned} \vec{U} &= \begin{bmatrix} \rho \\ \rho u \\ \rho v \\ \rho E \\ x_a \\ x_b \\ y_a \\ y_b \\ x \\ y \end{bmatrix}; \qquad \vec{F} = \begin{bmatrix} \rho u \\ \rho u^2 + p \\ \rho uv \\ \rho uE + pu \\ 0 \\ 0 \\ 0 \\ 0 \\ 0 \\ 0 \end{bmatrix} \\ \text{and} \\ \vec{G} &= \begin{bmatrix} \rho v \\ \rho uv \\ \rho v^2 + p \\ \rho vE + pv \\ 0 \\ 0 \\ 0 \\ 0 \\ 0 \\ 0 \end{bmatrix}; \qquad \vec{H} = \begin{bmatrix} 0 \\ 0 \\ 0 \\ 0 \\ 0 \\ 0 \\ 0 \\ 0 \\ 0 \\ 0 \end{bmatrix} \end{aligned}\right\} \qquad (5)$$

The last six equations are trivial and contain no unknowns. The eigenvalues of the Jacobian matrices are

$$\lambda = u,\ u \pm c,\ u$$

$$\beta = v,\ v \pm c,\ v$$

Thus we have recovered the familiar Eulerian description of the two-dimensional gasdynamic equations. If we set the mesh velocities to a nonzero constant, we obtain a system of equations very similar to the Eulerian description except for the convective velocities. Let u_m = constant, v_m = constant. This results in $x_a = 1$, $y_b = 1$, $x_b = 0$, $y_b = 0$, and $J = 1$, since we have $x = u_m(t - t_0) + a$ and $y = v_m(t - t_0) + b$. The system of equations becomes

$$\left.\begin{aligned} \vec{U} &= \begin{bmatrix} \rho \\ \rho u \\ \rho v \\ \rho E \\ x_a \\ x_b \\ y_a \\ y_b \\ x \\ y \end{bmatrix}; \qquad \vec{F} = \begin{bmatrix} \rho(u - u_m) \\ \rho u(u - u_m) + p \\ \rho v(u - u_m) \\ \rho E(u - u_m) + pu \\ 0 \\ 0 \\ 0 \\ 0 \\ 0 \\ 0 \end{bmatrix} \\ \text{and} \\ \vec{G} &= \begin{bmatrix} \rho(v - v_m) \\ \rho u(v - v_m) \\ \rho v(v - v_m) + p \\ \rho E(v - v_m) + pv \\ 0 \\ 0 \\ 0 \\ 0 \\ 0 \\ 0 \end{bmatrix}; \qquad \vec{H} = \begin{bmatrix} 0 \\ 0 \\ 0 \\ 0 \\ 0 \\ 0 \\ 0 \\ 0 \\ 0 \\ 0 \end{bmatrix} \end{aligned}\right\} \tag{6}$$

Again the last six equations are trivial. The eigenvalues now become

$$\lambda = (u - u_m),\ (u - u_m) \pm c,\ (u - u_m)$$

$$\beta = (v - v_m),\ (v - v_m) \pm c,\ (v - v_m)$$

We have gained the flexibility of controlling the magnitude and sign of the eigenvalues with no extra computational effort beyond the regular Eulerian description. However difficulties can arise at the boundaries.

Parametric system.- Suppose we do not require that initially $x = a$ and $y = b$, and let u_m, v_m be arbitrary; a parametric system (ref. 7) is then obtained. For comparison with the Eulerian system assume $u_m = v_m \equiv 0$. We then obtain

$$\left.\begin{aligned} \vec{U} &= \begin{bmatrix} J\rho \\ J\rho u \\ J\rho v \\ J\rho E \end{bmatrix} \quad ; \quad \vec{F} = \begin{bmatrix} J\rho u^M \\ J\rho u u^M + y_b p \\ J\rho v u^M - x_b p \\ J(\rho E + p)u^M \end{bmatrix} \\ \vec{G} &= \begin{bmatrix} J\rho v^M \\ J\rho u v^M - y_a p \\ J\rho v v^M + x_a p \\ J(\rho E + p)v^M \end{bmatrix} ; \text{ and } \vec{H} = \begin{bmatrix} 0 \\ 0 \\ 0 \\ 0 \end{bmatrix} \end{aligned}\right\} \tag{7}$$

The last six equations are the same as in equation (6) and are not shown. The eigenvalues of the Jacobian matrices are

$$\lambda = u^M,\ u^M \pm \frac{c}{J}\sqrt{x_b^2 + y_b^2}\ ,\ u^M$$

and

$$\beta = v^M,\ v^M \pm \frac{c}{J}\sqrt{x_a^2 + y_a^2}\ ,\ v^M$$

This set of equations is the transformed Euler equations in conservative form, where the usual notation is $a \equiv \xi$ and $b \equiv \eta$ with $\xi = \xi(x,y)$ and $\eta = \eta(x,y)$ being arbitrary.

Lagrangian system.- The Lagrangian description is obtained by setting $u_m = u$ and $v_m = v$, that is, the mesh moves with the fluid.

$$\vec{U} = \begin{bmatrix} J\rho \\ J\rho u \\ J\rho v \\ J\rho E \\ x_a \\ x_b \\ y_a \\ y_b \\ x \\ y \end{bmatrix} \quad ; \quad \vec{F} = \begin{bmatrix} 0 \\ y_b p \\ -x_b p \\ p(y_b u - x_b v) \\ -u \\ 0 \\ -v \\ 0 \\ 0 \\ 0 \end{bmatrix} \tag{8}$$

(Continued)

$$\vec{G} = \begin{bmatrix} 0 \\ -y_a p \\ x_a p \\ p(-y_a u + x_a v) \\ 0 \\ -u \\ 0 \\ -v \\ 0 \\ 0 \end{bmatrix}; \quad \vec{H} = \begin{bmatrix} 0 \\ 0 \\ 0 \\ 0 \\ 0 \\ 0 \\ 0 \\ 0 \\ -u \\ -v \end{bmatrix} \qquad (8) \text{ (Concluded)}$$

Here only the first equation is trivial and states that the mass of an element of volume $\Delta a\, \Delta b$ remains constant. The eigenvalues of the Jacobian matrices are

$$\lambda_{1,2,3,4} = 0, \pm \frac{c}{J} \sqrt{y_b^2 + x_b^2}, 0$$

$$\lambda_{5,\ldots,10} = 0$$

and

$$\beta_{1,2,3,4} = 0, \pm \frac{c}{J} \sqrt{y_a^2 + x_a^2}, 0$$

$$\beta_{5,\ldots,10} = 0$$

The Lagrangian description of the gasdynamic equations in three dimensions is similar to the two-dimensional case. It is given in appendix B.

The eigenvalues of the Lagrangian system are not directly dependent on the flow velocities but depend strongly on the mesh configuration. The eigenvalues are identical, whether the gas is polytropic or isentropic, and whether only the first four equations of the system (8) are used to determine the Jacobian matrices $(4 \times 4)\ \partial\vec{F}/\partial\vec{U}$ and $\partial\vec{G}/\partial\vec{U}$ with x_a, x_b, y_a, and y_b held constant, or if the full system of eight equations is used to obtain the (8×8) Jacobian matrices.

Before we go into a discussion of the properties and modifications of the Lagrangian system (eq. (8)), we will discuss the function of eigenvalues in finite difference methods. It is well known that a system of one-dimensional hyperbolic equations can be decoupled. If

$$U_t + [\vec{F}(\vec{U})]_a = 0$$

then

$$\vec{U}_t + A\vec{U}_a = 0$$

where

$$A = \frac{\partial \vec{F}}{\partial \vec{U}}$$

is the Jacobian matrix. We can now find a similarity transformation T which will diagonalize A, namely

$$T^{-1} A T = \begin{pmatrix} C_1 & & & \\ & C_2 & & 0 \\ & & \ddots & \\ 0 & & & C_n \end{pmatrix} \equiv C$$

The C_i's are the eigenvalues of the matrix A and are real for a hyperbolic system. The system becomes $(T^{-1}U_t) + T^{-1}AT(T^{-1}U_a) = 0$. Assume that T can be brought under the differentiation (true, in general, only for the linearized case) and set $u = T^{-1}U$ to obtain

$$\vec{u}_t + C\vec{u}_a = 0$$

The system is now decoupled

$$(u_i)_t + C_i(u_i)_a = 0$$

We now solve this system by a Lax-Wendroff scheme. The truncated form of the actual differential equation, termed the modified equation by Warming and Hyett (ref. 8), being solved by the finite difference scheme is for constant C

$$(u_i)_t + C_i(u_i)_a + \frac{C_i}{6}(\Delta a^2 - C_i^2\,\Delta t^2)(u_i)_{aaa}$$

$$+ \frac{C_i^2\,\Delta t}{8}(\Delta a^2 - C_i^2\,\Delta t^2)(u_i)_{aaaa} + O\left[C_i^n\left(\Delta a^2 - C_i^2\,\Delta t^2\right)\right] = 0$$

where Δa, Δt are the spatial and temporal step used to discretize the system. The Courant-Friedrich-Lewy number $CFL = C\Delta t/\Delta a \leq 1$ for stability of the scheme. If $CFL = 1$, the numerical scheme solves the original differential equation exactly.

Unfortunately, for a system, the C_i's are not constant, thus the $CFL = 1$ condition can be satisfied for only one equation; the others will introduce truncation errors. For the Lagrangian system, however, the eigenvalues can be adjusted by an appropriate mesh configuration. We now choose the mesh points so that (the signs of the eigenvalues are irrelevant)

$$\frac{c}{J}\sqrt{x_b^2 + y_b^2} = \frac{c}{J}\sqrt{x_a^2 + y_a^2} \equiv \lambda = \text{constant}$$

for all points in the computational domain. The modified equation now becomes

$$(u_i)_t = \lambda(u_i)_a + \frac{\lambda}{6}(\Delta a^2 - \lambda^2\Delta t^2)(u_i)_{aaa}$$

$$+ \frac{\lambda^2\Delta t}{8}(\Delta a^2 - \lambda^2\Delta t^2)(u_i)_{aaaa} + 0\left[\lambda^n\left(\Delta a^2 - \lambda^2\Delta t^2\right)\right] = 0$$

Setting the time step to the maximum allowable $\Delta t = \Delta a/\lambda$ results in

$$(u_i)_t + \lambda(u_i)_a = 0$$

In other words, the finite difference scheme solves the system of partial differential equations exactly. Two sources of error can still occur; namely, the inaccuracies in determining the mesh configuration and nonlinearity. The above analysis is for the linear case only. For the nonlinear case such as the inviscid gasdynamic equations, the above procedure of mesh adjustment will increase the accuracy of the numerical scheme by at least one order. This can be seen from Lerat and Peyret's analysis of the numerical solution of the inviscid Burger's equation by a generalized Lax-Wendroff scheme.

The above ideas are still in flux and no numerical verifications have been made. This is the end of the digression and now some properties and variations of the Lagrangian system (8) will be given.

Jump conditions for Lagrangian system.- Let $\sigma(a,b,t) = 0$ define a discontinuity surface in the Lagrangian space, then the jump conditions of system (8) are

$$[\vec{U}]\frac{\partial\sigma}{\partial t} + [\vec{F}]\frac{\partial\sigma}{\partial a} + [\vec{G}]\frac{\partial\sigma}{\partial b} = 0 \tag{9}$$

where [f] indicates the jump in the value of f in crossing the discontinuity surface $\sigma = 0$. The last two equations of system (8) are not included since they do not enter in the solution of the previous eight equations.

Total enthalpy form of the energy equation.- Consider the energy equation

$$[\rho JE]\frac{\partial\sigma}{\partial t} + [Jpu^M]\frac{\partial\sigma}{\partial a} + [Jpv^M]\frac{\partial\sigma}{\partial b} = 0$$

or setting on

$$u^M\frac{\vec{a}}{|a|} + v^M\frac{\vec{b}}{|b|} = \vec{q}^M$$

$$\left[(\rho JE\frac{\partial\sigma}{\partial t} + Jp\vec{q}^M\cdot\nabla\sigma)\right] = 0$$

We have

$$\frac{\partial \sigma}{\partial t} = \frac{\partial \sigma}{\partial a}\frac{\partial a}{\partial t}\bigg|_{\sigma} + \frac{\partial \sigma}{\partial b}\frac{\partial b}{\partial t}\bigg|_{\sigma}$$

and

$$\frac{da}{dt}\bigg|_{\sigma} = u_{\sigma}\frac{\partial a}{\partial x} + v_{\sigma}\frac{\partial a}{\partial y} + \frac{\partial a}{\partial t}\bigg|_{\sigma} = 0$$

hence

$$\frac{\partial a}{\partial t}\bigg|_{\sigma} = -u_{\sigma}\frac{\partial a}{\partial x} - v_{\sigma}\frac{\partial a}{\partial y}$$

and similarly for

$$\frac{\partial b}{\partial t}\bigg|_{\sigma} = -u_{\sigma}\frac{\partial b}{\partial x} - v_{\sigma}\frac{\partial b}{\partial y}$$

The Cartesian velocity components of the discontinuity surface in the Lagrangian coordinate system are u_σ and v_σ. Substituting into $\partial\sigma/\partial t$ results in

$$\frac{\partial \sigma}{\partial t} = -\left(\frac{y_b u_\sigma - x_b v_\sigma}{J}\right)\frac{\partial \sigma}{\partial a} - \left(\frac{-y_a u_\sigma + x_a v_\sigma}{J}\right)\frac{\partial \sigma}{\partial b}$$

or

$$\frac{\partial \sigma}{\partial t} = -u_\sigma^M \frac{\partial \sigma}{\partial a} - v_\sigma^M \frac{\partial \sigma}{\partial b}$$

$$= -\vec{q}_\sigma^M \cdot \nabla\sigma \qquad (10)$$

where u_σ^M and v_σ^M are the Lagrangian (moving mesh) components of the discontinuity surface in the Lagrangian coordinate system. The discontinuity velocity in the Lagrangian system can be expressed in terms of Cartesian velocities, that is,

$$\vec{q}_\sigma^M = \vec{q}_{\sigma c}^M - \vec{q}^M$$

where $\vec{q}_{\sigma c}^M$, $\vec{q}^M$ are the discontinuity and mesh velocity, respectively, in the Cartesian system given, however, in terms of the Lagrangian components. The mesh velocity is, of course, the fluid velocity. Hence

$$\frac{\partial \sigma}{\partial t} = \vec{q}^M \cdot \nabla\sigma - \vec{q}_{\sigma c}^M \cdot \nabla\sigma$$

The energy jump condition is now

$$\left[J\rho\left(E + \frac{p}{\rho}\right)\frac{\partial\sigma}{\partial t} + Jp\,\vec{q}^{\,M}_{\sigma c} \cdot \nabla\sigma\right] = 0 \tag{11}$$

In terms of the differential equation this becomes

$$\frac{\partial}{\partial t} J\rho\left(E + \frac{p}{\rho}\right) + \frac{\partial}{\partial a}\left(Jp\,u^{M}_{\sigma c}\right) + \frac{\partial}{\partial b}\left(Jp\,v^{M}_{\sigma c}\right) = 0 \tag{12}$$

If the flow is stationary, $\vec{q}^{\,M}_{\sigma c} = 0$, the energy equation reduces to

$$\frac{\partial}{\partial t} J\rho\left(E + \frac{p}{\rho}\right) = 0 \tag{13}$$

The equation shows that the total enthalpy $h_t = E + p/\rho$ is constant along a particle path if the flow is stationary. Since equation (13) was derived using the proper jump conditions (eq. (9)), we have the condition that the total enthalpy is not discontinuous across $\sigma = 0$, that is,

$$[h_t] = 0 \tag{14}$$

for steady flows, even for Lagrangian systems which always contain time derivatives.

Pressure form of energy equation.- The energy equation of system (8) can be reduced to

$$\frac{\partial}{\partial t}\left(J^{\gamma}p\right) = 0 \tag{15}$$

by combining the equation of system (8), assuming the polytropic (not isentropic) gas relation

$$E = \frac{p}{(\gamma - 1)\rho} + \frac{1}{2}(u^2 + v^2)$$

and noting that

$$\frac{\partial J}{\partial t} - \frac{\partial}{\partial a}\left(y_b u - x_b v\right) - \frac{\partial}{\partial b}\left(-y_a u + x_a v\right) = 0$$

Another form of equation (15) is obtained by combining it with the continuity equation and the state equation relating the entropy in terms of the pressure and density for polytropic gases

$$s = s_o + C_v \ln\frac{p}{\rho^{\gamma}}$$

to obtain

$$\frac{\partial}{\partial t}(\rho J s) = 0 \tag{16}$$

The physical meaning of the energy equation (15) is that the entropy, s, of a fluid particle is a constant for adiabatic flows. This is as expected if the flow is continuous. Unfortunately, equations (15) or (16) do not satisfy the jump conditions (eq. (9)). The proper form of equation (16) must be derived from the entropy transport equation which is not included in the Euler Equations of gasdynamics. The Lagrangian form of the entropy equation for adiabatic flows is

$$\frac{\partial}{\partial t}(\rho J s) \geq 0 \tag{17}$$

which has the jump condition

$$[\rho J s]\frac{\partial \sigma}{\partial t} \geq 0 \tag{18}$$

which is quite different from that of equation (16). However, equation (15) or (16) is still useful for transonic flows where the entropy changes are of $0(\Delta p^3)$.

Lagrangian Coordinates

The Lagrangian coordinates serve to identify the fluid particles. At some initial time a distribution of particles (or cells) is chosen in the physical plane (fig. 1). Each particle is identified by the Lagrangian coordinates (a_i, b_j). For simplicity we set $a_i = i$, and $b_j = j$ where $i = 1,2,\ldots,L$ and $j = 1,2,\ldots,M$ with the total number of cells being $L \times M$. The Lagrangian plane will then consist of unit square cells with any boundaries appearing as slits as in figure 1. Single or multielement boundaries are possible. Unlike the procedure followed by Lamb (ref. 7), the initial distribution of points is not uniform, that is, $a \neq k_1 x$, $b \neq k_2 y$, k_1, k_2 are constants. This nonuniform distribution allows the particles to be clustered around boundaries and be identified by integer values, which simplify the numerics.

Boundary Conditions

There are four types of boundary conditions to be considered: inflow, outflow, free stream or far field, and impermeable surface condition. All boundary conditions are first predicted by the FCT method and then the following procedures are utilized to correct the predicted values. This is very similar to Abbett's procedure (ref. 9), except his is restricted to steady supersonic flows. To predict the boundary terms by the FCT method without turning the flux limiter off, the flow field is linearly extrapolated two points beyond the boundary. The procedure will be derived for two dimensions but it is also valid for three-dimensional flows.

The inflow boundary condition is simple. The dependent variables of system (8) are set to the specified inflow conditions. The outflow boundary is not so simple. If the flow is supersonic, then the particles along with their properties are allowed to flow out undisturbed, that is, a linear

extrapolation will do and will not disturb the upstream conditions. If the outflow is subsonic, then some outflow boundary conditions are required to set the dependent variables of system (8). What these outflow boundary conditions should be is yet unknown.

The far-field boundary condition will be treated similarly to the impermeable surface boundary and this requires that some analytic representation of the far-field streamline be given. Let both the far-field streamline and the surface streamline be given by

$$y = f(x) \tag{19a}$$

We have used the term streamline loosely. It includes particle paths and thus the streamlines coincide with the Lagrangian coordinate b = constant. Differentiation (eq. (19a)) with respect to time obtains

$$y_t = f'(x)x_t \tag{19b}$$

We assume that $f(x)$ is differentiable as many times as necessary. From the last two equations of system (8) we have

$$x_t = u \tag{19c}$$

$$y_t = v \tag{19d}$$

thus

$$v = f'(x)u \tag{19e}$$

Differentiating equation (19a) with respect to "a" and equation (19b) with respect to "t" obtains

$$y_a = f'(x) \cdot x_a \tag{20a}$$

$$v_t = f'(x) \cdot u_t + f''(x) \cdot u^2 \tag{20b}$$

The two momentum equations of system (8) are cross multiplied and summed to eliminate the p_b terms to obtain

$$(\rho J u)_t + \frac{\rho J}{1 + f'^2}\left(\frac{p_a}{x_a \rho} + u^2 f' f''\right) = 0$$

where use has been made of equations (20a) and (20b). The time may now be eliminated by the x-momentum equation of system (8) to obtain

$$x_a(1 + f'^2)p_b - (x_b + y_b f')p_a + (\rho J)u^2 f'' = 0 \tag{21}$$

This is the normal momentum equation in the Lagrangian coordinates. Since we are solving system (8) by a time-splitting procedure, the boundary values along the two boundary streamlines are required only during the "b" sweep. Hence we are only solving part of system (8); namely,

$$\frac{\partial \vec{U}}{\partial t} + \frac{\partial \vec{G}}{\partial b} + \vec{H} = 0$$

Only $\vec{G}$ is required along the two streamlines. $\vec{G}$ is determined by u, v, x_a, y_a, and p. We have equations (19a), (19b), (20a), and (21) available. To obtain the remaining relation we need to specialize the equations to steady or unsteady and isentropic or polytropic flows.

Polytropic unsteady.- If the flow is unsteady and polytropic, then we simply extrapolate x and u to surface, y is computed and x_a, x_b and y_b are obtained by second order accurate finite differencing, either central or one-sided as required. The p_b of equation (21) is approximated by a one-sided difference and the p_a by a central difference to obtain a scalar tridiagonal system for the unknown p at the surface. The density is obtained from the continuity equation

$$\rho = \frac{(\rho J)}{(x_a y_b - x_b y_a)}$$

v from equation (19e) and E from the equation of state.

Polytropic steady.- If the flow is steady, then use is made of the steady-state version of the energy equation

$$h_t = \frac{\gamma p}{(\gamma - 1)\rho} + \frac{u^2(1 + f'^2)}{2} = \text{constant} \qquad (22)$$

Substituting this into the normal momentum equation to eliminate the u^2 term obtains

$$x_a(1 + f'^2)pb - (x_b + y_b f')\, pa - \frac{2\gamma J f''}{(\gamma - 1)(1 + f'^2)}\, p = \frac{2(pJ)f''h_t}{(1 + f'^2)} \qquad (23)$$

The same procedure may now be followed as previously except u is not extrapolated. Once p, x_a, y_a, x_b, and y_b have been obtained, u and v result from equations (22) and (19d), respectively. The determination of E is also the same as previously described.

Transonic unsteady or steady.- The only additional simplification in transonic flows is that it can be assumed to be isentropic, thus

$$p = k\rho^{\gamma} \qquad (24)$$

The density is now computed from this relation and y_b is computed from

$$y_b = \left[\frac{(J\rho)}{\rho} - x_b y_a\right] \Big/ x_a$$

to keep the system consistent.

Parametric form of $y = f(x)$.- If the bounding streamline behaves such that f' and/or f'' do not exist, then equations (19a,b) and (20a,b) are replaced by their parametric representation. Let the arc length along the curve $y = f(x)$ be given by σ, then equations (19a) and (19b) become

$$\left.\begin{aligned} y &= \eta(\sigma) \\ x &= \xi(\sigma) \end{aligned}\right\} \tag{19a'}$$

$$v \cdot x_\sigma = u \cdot y_\sigma \tag{19b'}$$

and equations (20a) and 20b) become

$$y_a x_\sigma = x_a y_\sigma \tag{20a'}$$

$$x_\sigma^3 v_t = y_\sigma x_\sigma^2 u_t + (x_\sigma y_{\sigma\sigma} - y_\sigma x_{\sigma\sigma})\, u^2 \tag{20b'}$$

Equation (19a') is the parametric counterpart to equation (19a) and η and ξ are given continuous and smooth functions of σ. We require that the function be smooth so that $y_{\sigma\sigma}$ and $x_{\sigma\sigma}$ remain finite. The continuity condition guarantees the boundedness of $y_\sigma^{\sigma\sigma}$ and x_σ. These restrictions mean that the streamline is continuous without any kinks or sharp corners.

III. NUMERICAL SOLUTION METHODS

The numerical solution of system (8) is obtained by an explicit hyperbolic differential equation solver. Of the ten equations of system (8) only nine need by solved by the D.E. solver. Unfortunately, most of the present numerical schemes have been devised for Eulerian systems and it does not necessarily follow that they will be efficient for Lagrangian systems. The procedures devised for Lagrangian or Euler-Lagrangian systems, such as by the Los Alamos group (ref. 6) are not applicable to system (8). Most of the various Lagrangian procedures devised by the Los Alamos group and others operate on the Cartesian space and not the Lagrangian space as required by system (8). We also required that any discontinuities in the flow field be captured accurately without excessive and spurious nonphysical oscillations by the numerical procedure, as we did not want to add the additional complications of shock fitting procedures.

We finally required that a time-step splitting procedure be used so that the number of equations to be solved during each sweep in the two spatial directions is reduced to six. This requirement is necessary to make the numerical computation in the Lagrangian system competitive with that in the

Eulerian system. The Eulerian system requires that four equations be solved during each sweep. For these reasons several different numerical schemes were tried of which only four will be given here. They are the MacCormack, generalized Lax-Wendroff, Shasta flux corrected transport FCT, and the "fourth-order phase error" FCT schemes. All schemes will be given for the one-dimensional, nonlinear, hyperbolic system $\vec{f}_t + [F(\vec{f})]_x + \vec{S} = 0$. Here $\vec{f}(x,t)$ is a column vector of m components and the Jacobian matrix $A = \vec{F}'(\vec{f})$ has m real and distinct eigenvalues $\lambda(\vec{f})$.

MacCormack and Generalized Lax-Wendroff Schemes

The MacCormack schemes are special cases of the generalized Lax-Wendroff schemes devised by Lerat and Peyret (ref. 10), thus only the latter schemes will be given. The schemes are given in a predictor-corrector form:

$$\left.\begin{aligned} \text{P:}\quad & \tilde{f}_i = (1-\beta)\, f_i^n + \beta\, f_{i+1}^n - \alpha\sigma\,(F_{i+1}^n - F_i^n) - \alpha\Delta t S_i^n \\ \text{C:}\quad & f_i^{n+1} = f_i^n - \frac{\sigma}{2\alpha}\Big[(\alpha-\beta)\,F_{i+1}^n + (2\beta-1)\,F_i^n \\ & \qquad + (1-\alpha-\beta)\,F_{i-1}^n + \tilde{F}_i - \tilde{F}_{i-1}\Big] - \frac{\Delta t}{2\alpha}\tilde{S}_i \end{aligned}\right\} \qquad (1)$$

where

$t = n\Delta t$

$x = i\Delta x$

$\sigma = \Delta t/\Delta x$

α,β = two arbitrary parameters with $\alpha \neq 0$

The predictor $\tilde{f}_i$ is an approximation to the solution at $x = (i + \beta)\,\Delta x$ and $t = (n + \alpha)\,\Delta t$. The schemes are three-point, second-order accurate for all values of $\alpha \neq 0$ and β, and stable for $\lambda_{max}\sigma \leq 1$. Setting $\alpha = 1$ and $\beta = 0, 1$ yields the two MacCormack schemes. Lerat and Peyret determined that the optimum values are $\alpha = 1 + \sqrt{5}/2 (=2.118)$ and $\beta = 1/2$ using the inviscid Burgers equation as the model system in their analysis of the truncation errors. They were not able to analyze the truncation errors using the full Euler equations. If the scheme (1) is applied to a linear system $f_t + cf_x = 0$, then the actual differential equation, called modified equation by Warming and Hyett (ref. 8), solved by the scheme is

$$f_t + cf_x + \frac{c}{6}(\Delta x^2 - c^2\Delta t^2)\, f_{xxx} + \frac{c^2\Delta t}{8}(\Delta x^2 - c^2\Delta t^2)\, f_{xxxx} + \ldots = 0$$

Nothing can be said about the parameters α,β from linear analysis. This is not the case, however, for the nonlinear system as shown by Lerat and Peyret. For our Lagrangian system, both the MacCormack schemes and the optimum Lerat and Peyret scheme were tried with equally disappointing results to be shown

in section IV. The introduction of an artificial viscosity to the scheme (1) did not improve the results, in fact, the results were even slightly more degraded.

Shasta Flux Corrected Transport Algorithm

The flux corrected transport algorithms developed by Boris and Book (ref. 11) require that the nonlinear hyperbolic system be written in the form

$$\vec{f}_t + (u\vec{f})_x + \vec{S} = 0$$

where u is the convective velocity transporting $\vec{f}$. It is similar to the previous form of the hyperbolic system. Thus we have for the one-dimensional Euler Equation

$$\vec{f} = \begin{bmatrix} \rho \\ \rho u \\ e \end{bmatrix}; \text{ and } \vec{s} = \begin{bmatrix} 0 \\ p_x \\ (pu)_x \end{bmatrix}$$

where for a polytropic ideal gas

$$e = \frac{p}{\gamma-1} + \frac{\rho u^2}{2}$$

The Shasta FCT scheme (ref. 12) is as follows. Let f_i^0, u_i, and S_i be given for $i = 1,2, \ldots, N$. First, the untransported and a diffused solution are computed

$$f_{i+\frac{1}{2}}^0 = \frac{1}{8}\left(f_{i+1}^0 - f_i^0\right)$$

$$f_i^D = f_i^0 + f_{i+\frac{1}{2}}^0 - f_{i-\frac{1}{2}}^0$$

where the superscripts given here and later will stand for

0 - initial
D - diffused
T - transported
TD - diffused and transported
C - corrected

Now determine the convective transport factors

$$\varepsilon_i^{\pm} = \frac{1}{2} \pm u_i\sigma$$

$$Q_i^+ = 1 - Q_i^- = \frac{\varepsilon_i^-}{\varepsilon_{i+1}^+ + \varepsilon_i^-}$$

and source terms for $S = \partial p/\partial x$

$$S_{i+\frac{1}{2}} = \sigma(p^0_{i+1} - p^0_i)$$

or if $S = p$, then

$$S_{i+\frac{1}{2}} = \frac{\Delta t}{2}\left(p^0_{i+1} + p^0_i\right)$$

The transported diffused solution is

$$f^{TD}_i = 4(Q^+_i)^2\, f^0_{i+\frac{1}{2}} - 4(Q^-_i)^2\, f^0_{i-\frac{1}{2}}$$

$$+ Q^+_i(f^0_i - S_{i+\frac{1}{2}}) + Q^-_i(f^0_i - S_{i-\frac{1}{2}})$$

The changes due to transport alone are

$$\delta f^T_i = f^{TD}_i - f^D_i$$

and differences in the diffused transported fluxes are

$$\delta f^{TD}_{i+\frac{1}{2}} = f^{TD}_{i+1} - f^{TD}_i$$

and initial fluxes are modified by the convective transport

$$f^T_{i+\frac{1}{2}} = f^0_{i+\frac{1}{2}} + \frac{1}{8}\left(\delta f^T_{i+1} - \delta f^T_i\right)$$

These fluxes are now corrected by the nonlinear flux limiter

$$f^C_{i+\frac{1}{2}} = Sgn \cdot Max\left[0,\ Min\left(Sgn \cdot \delta f^{TD}_{i-\frac{1}{2}},\ |f^T_{i+\frac{1}{2}}|,\ Sgn \cdot \delta f^{TD}_{i+\frac{3}{2}}\right)\right]$$

where

$$Sgn = sign(f_{i+\frac{1}{2}})$$

The final flux corrected transported solution at the new time step is obtained by

$$f^1_i = f^{TD}_i - \left(f^C_{i+\frac{1}{2}} - f^C_{i-\frac{1}{2}}\right)$$

The corrected flux $f^C_{i+\frac{1}{2}}$ has four different possible values; namely, 0, $\delta f^{TD}_{i-\frac{1}{2}}$, $f^T_{i+\frac{1}{2}}$, or $\delta^{TD}_{i+\frac{3}{2}}$. Therefore, the final time corrected transport solution has a total of 16 different finite difference representations. We will analyze only the two most prevalent ones; namely, the cases for

$$f^c_{i+\frac{1}{2}} = f^c_{i-\frac{1}{2}} = 0$$

and

$$f^c_{i+\frac{1}{2}} = f^T_{i+\frac{1}{2}} \ , \ f^c_{i-\frac{1}{2}} = f^T_{i-\frac{1}{2}}$$

To analyze the Shasta FCT scheme we will drop the source terms and assume the u_i's to be constant = c. Define $\alpha = u\sigma$. For the first case ($f^c_{i\pm\frac{1}{2}} = 0$) we have

$$f^1_i = f^{TD}_i$$

$$= f^0_i - \frac{1}{2}\alpha\left(f^0_{i+1} - f^0_{i-1}\right) + \left(\frac{1}{2}\alpha^2 + \frac{1}{8}\right)\left(f^0_{i+1} - 2f^0_i + f^0_{i-1}\right)$$

which has the modified equation

$$f_t + cf_x - \frac{\sigma\Delta x}{8} f_{xx} + \frac{c}{6}\left(\frac{\Delta x^2}{4} - c^2\Delta t^2\right) f_{xxx} +$$

$$+ \left[\frac{c^2\Delta t}{8}\left(\frac{\Delta x^2}{4} - c^2\Delta t^2\right) - \frac{\sigma\Delta x}{32}\left(\frac{\Delta x^2}{12} - c^2\Delta t^2\right)\right] f_{xxxx} + \ldots = 0$$

The modified equation shows that for this case, that is, null flux correction, the scheme is only first-order accurate. For the second case ($f^c_{i\pm\frac{1}{2}} = f^T_{i\pm\frac{1}{2}}$) we have

$$f^1_i = f^{TD}_i - \left(f^T_{i+\frac{1}{2}} - f^T_{i-\frac{1}{2}}\right)$$

$$= f^0_i - \alpha\left[\frac{1}{4}\left(\frac{f^0_{i+1} - f^0_{i-1}}{2}\right) + \frac{3}{4}\left(\frac{2f^0_{i-2} - 16f^0_{i-1} + 16f^0_{i+1} - 2f^0_{i+2}}{24}\right)\right]$$

$$+ \frac{\alpha^2}{2}\left[-\frac{1}{2}\left(f^0_{i+1} - 2f^0_i + f^0_{i-1}\right) + \frac{3}{2}\left(\frac{-f^0_{i+2} + 16f^0_{i+1} - 30f^0_i + 16f^0_{i-1} - f^0_{i-2}}{12}\right)\right]$$

The modified equation is

$$f_t + cf_x + \frac{c}{6}\left(\frac{\Delta x^2}{4} - c^2\Delta t^2\right) f_{xxx} +$$

$$\frac{c^2\Delta t}{8}\left(\Delta x^2 - c^2\Delta t^2\right) f_{xxx} + \ldots = 0$$

Here the scheme has second-order accuracy and this modified equation shows that the dispersion error is approximately only one-fourth the dispersion of the Lax-Wendroff scheme as shown by the coefficients of the f_{xxx} term of

the modified equations of the two schemes. This is one of the reasons for the improved performance of the FCT scheme over the generalized Lax-Wendroff schemes. The standard Fourier (Von Neumann) stability analysis of the two methods confirms this conclusion. Figure 2 shows the amplification factor $|\xi|$ and dispersion (or phase) error ϕ/ϕ_e for the two methods at two CFL numbers. For both CFL numbers shown the dispersion error is substantially less for the FCT method. Another reason is that the flux limiter sets the flux correction $f^c_{i+\frac{1}{2}}$ to zero near discontinuities and thus insures that the solution remains monotonic near these discontinuities, where the Lax-Wendroff schemes usually show spurious nonphysical oscillations. The FCT scheme has only first-order accuracy in this situation. However, this condition usually occurs only in a small neighborhood of the discontinuity, so the FCT scheme is essentially second-order accurate over most of the computational domain.

The condition for stability is $|u|_{max}\sigma \leq 1$ and for monotonicity is $|u|_{max}\sigma \leq \sqrt{3}/2$.

Although it is not immediately apparent from the scheme given, the essential features of the FCT scheme are:

1. The conserved quantities f^0_i are changed by the convective transport and source terms. Enough nonphysical damping is provided so that the solution remains monotonic if initially monotonic.

2. Flux antidiffusion terms $f^T_{i+\frac{1}{2}}$ are computed so that the excessive damping of step one can be eliminated where not needed.

3. However, before the solution is antidiffused, the antidiffusion terms $f^T_{i+\frac{1}{2}}$ must be modified to $f^c_{i+\frac{1}{2}}$ by the nonlinear flux limiter to preserve the monotonicity of the antidiffused solution of step one.

The effect of these three steps of the Shasta FCT scheme is shown graphically for a one-dimensional Riemann bursting diaphragm problem in figures 3a, b, c. These figures show the pressure profile at the initial state and at a later time. The first figure shows the solution after the diffused transport step. This solution is smooth and monotonic. The antidiffused solution without the flux limiter is shown in figure 3b. Large overshoots occur near the shock which has been steepened from that of the first step. The last figure shows the final solution where the antidiffusion fluxes have been limited by the nonlinear flux limiter. The solution is nearly monotonic and most of the shock jump occurs over two cells compared to six or seven cells after the first step. The final solution is not quite monotonic, and that is due to the pressure being determined from the three conserved quantities: density, momentum, and total energy, all three of which are computed monotonically by the FCT scheme. The three phases of the FCT algorithm are more obvious in the third order FCT described below.

Third-Order FCT

The third-order FCT scheme is the latest and most accurate scheme devised by Boris and Book (ref. 11) who call it the "Fourth-Order Phase Error" FCT.

The procedure shown here differs from that of Boris and Book in two respects: (1) the computational mesh is rectangular and fixed but not necessarily uniformly spaced, and (2) the cell node positions are shifted by 1/2 cell width from that of Boris and Book. The notation of the mesh configuration is shown in figure 4.

Figure 4 has N grid points and N - 1 interfaces. The interface positions are denoted by

$$r_{i+\frac{1}{2}} = \frac{1}{2}\left(r_i + r_{i+1}\right) \qquad i = 1, \ldots, N-1$$

To determine the interface fluxes, we need the interface velocities

$$\delta u_{i+\frac{1}{2}} = \frac{1}{2}\left(u_i + u_{i+1}\right) \qquad i = 1, \ldots, N-1$$

and the interface conserved quantity

$$f^0_{i+\frac{1}{2}} = \frac{1}{2}\left(f^0_i + f^0_{i+\frac{1}{2}}\right) \qquad i = 1, \ldots, N-1$$

The transported f^T_i due to convection and source terms can now be computed

$$\Lambda^0_i f^T_i = \Lambda^0_i f^0_i - \Delta t\left(f^0_{i+\frac{1}{2}}\,\delta u_{i+\frac{1}{2}} - f^0_{i-\frac{1}{2}}\,\delta u_{i-\frac{1}{2}}\right) + \frac{\Delta t}{2}\left(p_{i+1} - p_{i-1}\right)$$

for $i = 2, \ldots, N-1$. And for $i = 1, N$

$$f^T_i = f^0_i$$

We assume that the source S is given by $\partial p/\partial x$. Extensions to other types of source terms are obvious. The cell volume is

$$\Lambda_i = \frac{1}{2}\left(r_{i+1} - r_{i-1}\right)$$

The diffused transport is now determined by

$$\Lambda_i f^{TD}_i = \Lambda_i f^T_i + \nu_{i+\frac{1}{2}}\Lambda_{i+\frac{1}{2}}\left(f^0_{i+1} - f^0_i\right) - \nu_{i-\frac{1}{2}}\Lambda_{i-\frac{1}{2}}\left(f^0_i - f^0_{i-1}\right)$$

for $i = 2, \ldots, N-1$, and set $f^{TD}_i = f^0_i$ for $i = 1, N$. The interface volumes are defined as

$$\Lambda_{i+\frac{1}{2}} = r_{i+1} - r_i \qquad \text{for } i = 1, \ldots, N-1$$

The diffusion coefficient will be defined later. The uncorrected antidiffusive fluxes are defined as

$$F_{i+\frac{1}{2}} = \mu_{i+\frac{1}{2}} \Lambda_{i+\frac{1}{2}} \left(f^T_{i+1} - f^T_i \right) \quad \text{for } i = 1, \ldots, N-1$$

where $\mu_{i+\frac{1}{2}}$ is the antidiffusion coefficient. The raw antidiffusive fluxes are now corrected.

$$F^c_{i+\frac{1}{2}} = \text{Sgn} \cdot \text{Max}\left\{0, \text{Min}\left[|F_{i+\frac{1}{2}}|, \text{Sgn} \cdot \Lambda_{i+1}\left(f^{TD}_{i+2} - f^{TD}_{i+1}\right), \text{Sgn} \cdot \Lambda_i \left(f^{TD}_i - f^{TD}_{i-1}\right)\right]\right\}$$

where

$$\text{Sgn} = \text{sign}\left(f^{TD}_{i+1} - f^{TD}_i\right)$$

for $i = 2, \ldots, N-2$. The corrected fluxes $F^c_{3/2}$ and $F^c_{N-\frac{1}{2}}$ are determined by the above relation, dropping the undefined terms outside the boundary. The final results are now obtained

$$f^1_i = f^{TD}_i - \frac{1}{\Lambda_i}\left(F^c_{i+\frac{1}{2}} - F^c_{i-\frac{1}{2}}\right)$$

for $i = 2, \ldots, N-1$. The diffusive and antidiffusive coefficients are

$$\nu_{i+\frac{1}{2}} = \frac{1}{6} + \frac{\epsilon^2_{i+\frac{1}{2}}}{3}$$

$$\mu_{i+\frac{1}{2}} = \frac{1}{6} - \frac{\epsilon^2_{i+\frac{1}{2}}}{6}$$

with

$$\epsilon_{i+\frac{1}{2}} = \delta u_{i+\frac{1}{2}} \frac{\Delta t}{2}\left(\frac{1}{\Lambda_i} + \frac{1}{\Lambda_{i+1}}\right)$$

These choices make the scheme third order accurate as shown below.

If we now assume that we have uniform mesh spacing so that $\Delta x = \Delta r = 1/2(r_{i+1} - r_{i-1}) = \Lambda_i$ and constant convective velocity $u_i = C$, then the modified equation of the scheme is

$$f_t + cf_x + \frac{\Delta x^2}{\Delta t}\left(\mu - \nu + \frac{\epsilon^2}{2}\right) f_{xx} + \frac{\epsilon \Delta x^3}{\Delta t}\left(\frac{1}{6} + \frac{\epsilon^2}{3} - \nu\right) f_{xxx}$$

$$+ \frac{\Delta x^4}{\Delta t}\left[\frac{\epsilon^4}{4} + \left(\frac{1}{6} - \nu\right)\epsilon^2 + \frac{\mu - \nu}{12} + \frac{(\mu - \nu)^2}{2}\right] f_{xxxx} + \ldots = 0$$

where ϵ is the CFL number = $C\Delta t/\Delta x$. With the above choices of ν and μ the modified equation becomes

$$f_t + cf_x + \frac{\Delta x^4}{24}\frac{\epsilon^2}{\Delta t}(\epsilon^2 - 1)f_{xxxx} + \ldots = 0$$

That is, the scheme is third order accurate, $0(\Delta x^4/\Delta t)$. In the neighborhoods of discontinuities the flux limiter essentially sets $\mu = 0$ and the scheme becomes accurate of $0(\Delta x^2/\Delta t)$. It can be shown that the CFL restriction for stability is $CFL \leq 1$ and for monotonicity also ≤ 1.

For nonlinear problems, both of the FCT algorithms require the solution to be advanced in two half-time steps to arrive at the final time $(n + 1)t$ where $\Delta t \leq \Delta x/\lambda_{max}$ to maintain the same order accuracy for nonlinear problems as for linear ones. This procedure is equivalent to the predictor-corrector steps of the Lax-Wendroff schemes.

Another comment is that for the Lagrangian system (8) there are no convective velocities and thus it might be argued that the FCT algorithms are not applicable for this system. However, the convective transport can be considered to be by the eigenvalues of the Jacobian matrix rather than the actual fluid convective velocity. For example, Boris and Book (ref. 11) argue that for a one-dimensional Eulerian system, the effective convective velocities are u, u, and $(1 + p/e)u$ for the continuity, momentum, and energy equations, respectively. Thus, even for a Lagrangian system, the energy transport is by the convective velocity $(p/e)u$. It is more valid, however, to consider the eigenvalues to be the effective transport velocities. Consider the Eulerian system in one dimension

$$f_t + w_x = 0$$

where

$$f = \begin{bmatrix} \rho \\ \rho u \\ e \end{bmatrix}; \qquad w = \begin{bmatrix} \rho u \\ \rho u^2 + p \\ (e + p)u \end{bmatrix}$$

Now define the Jacobian matrix $A = \partial w/\partial f$, to obtain

$$f_t + (Af)_x = 0$$

where we have used the homogeneous property of the Eulerian system (ref. 13). A similarity transformation T can now be defined so that Jacobian matrix A is diagonalized and $\tilde{f} = T^{-1}f$ where the $\tilde{f}_i$'s differ from the f_i's only by a constant factor, that is

$$D \equiv T^{-1}AT = \begin{pmatrix} u & 0 & 0 \\ 0 & u+c & 0 \\ 0 & 0 & u-c \end{pmatrix}$$

and $\tilde{f}_i = k_i f_i$. The system after some manipulation becomes

$$(T^{-1}f)_t + (DT^{-1}f)_x - (T_t^{-1}f + T_x^{-1}w) = 0$$

or

$$\tilde{f}_t + (D\tilde{f})_x + S = 0$$

where S are the source terms

$$S = -(T_t^{-1}f + T_x^{-1}w)$$

The inverse similarity transformation is

$$T^{-1} = \frac{\gamma(\gamma - 1)}{c^2}\begin{bmatrix} \frac{1}{\gamma - 1}\left(\frac{c^2}{\gamma - 1} - \frac{u^2}{2}\right) & \frac{u}{\gamma - 1} & -\frac{1}{\gamma - 1} \\ u\left(\frac{-uc}{\gamma - 1} + \frac{u^2}{2}\right) & \frac{uc}{\gamma - 1} - u^2 & u \\ \frac{e}{\rho}\left(\frac{uc}{\gamma - 1} + \frac{u^2}{2}\right) & -\frac{e}{\rho}\left(\frac{c}{\gamma - 1} + u\right) & \frac{e}{\rho} \end{bmatrix}$$

With this transformation we can compute $\tilde{f}$ to be $\tilde{f} = T^{-1}f \equiv f$, so the constant coefficients k_i are unity. The source terms are

$$S = \begin{bmatrix} 0 \\ \frac{\partial}{\partial x}\left\{\rho c\left[u - \frac{c}{\gamma}\right]\right\} \\ \frac{\partial}{\partial x}\left\{(\gamma - 1)\frac{\rho u^3}{2} - e[c + (\gamma - 1)u]\right\} \end{bmatrix}$$

Here we have a system, completely equivalent to the original system, which gives the proper jump conditions and which has the eigenvalues as the effective convective velocities. This shows that the convective terms of the Eulerian system play no major role in the FCT algorithms. Similarly for the Lagrangian systems, which have some nonzero eigenvalues, but zero convective velocities. The lack of convective velocities does not prohibit the use of the FCT algorithms.

IV. NUMERICAL RESULTS

In this section the numerical methods of section II are compared for a one-dimensional Riemann problem (bursting diaphragm). The most effective method will then be applied to a two-dimensional problem of the ordinary

oblique shock wave reflection off a channel wall. To check the boundary conditions, the Riemann problem consists of a shock tube with reflecting end walls. For the two-dimensional problem, the boundary procedures described in section II are used even for the case of straight walls where reflection principles would be much simpler.

The initial conditions and geometry of the Riemann problem are shown in figure 5. As a standard of comparison, this problem was solved in the Eulerian coordinates with the MacCormack scheme. Initially the pressure profile is a step function as in figure 6. After the burst a shock wave propagates to the right and a rarefaction wave to the left. At later times these two waves reflect off the end walls. The shock and rarefaction waves are resolved quite well except for the slight spike of the reflected shock wave and slight oscillation at the foot of the rarefaction wave. The spatial step $\Delta x = 0.002$ is quite small and good resolution is to be expected. Changing to the Lagrangian system with everything else fixed results in the solution shown in figure 7. The oscillations at the root of the expansion wave are larger and the spike at the reflected shock wave is much larger. The particles are at first equally spaced at $\Delta x = 0.002$ so the masses in each cell $(\rho J = \rho x_a)$ are not uniform initially. The temperature (p/ρ) profiles are shown in figure 7b.

If the initial particle distribution is such that we have equal mass in all the cells, then the results shown in figure 8 are obtained. Large oscillations trail from the shock waves. The expansion waves seem to be resolved better. Thus nothing is gained by adjusting the fluid cells to contain equal masses.

Relaxing the restriction of equal masses and using the generalized Lax-Wendroff method with the optimum values of the two arbitrary parameters of Lerat and Peyret (ref. 10) obtains a much improved solution (fig. 9). The oscillations at the shocks are much smaller, but the expansion wave oscillations are about the same as previously. Including an artificial dissipation of the Lapidus type (ref. 10) does not improve the solution as it does for an Eulerian calculation (fig. 10). Other values of the two parameters did not improve the results.

Somewhat improved results are obtained from the FCT method of Book, Boris and Hain (ref. 12). Figure 11 shows that the oscillations at the expansion wave and outgoing shock wave are gone. A spike appears at the reflected shock and also at the contact surface. The contact surface oscillations disappear if equal-mass fluid cells are chosen. The spike appears at the reflected shock since the flux limiter of the original FCT method is partially turned off at the boundaries.

All the methods tested tend to give comparable results with the FCT method giving slightly better results. However, all the cases considered so far have a very fine mesh distribution of $\Delta x \cong 0.002$ or 500 points. For two or three dimensions this is excessive. Reducing the number of points to 50 obtains quite different results. These results are shown in figures 12 through 15 for the optimum generalized Lax-Wendroff method for the Eulerian

coordinates and Lagrangian coordinates, and for the 1/8 (Shasta) FCT, and third order FCT method with Lagrangian coordinates, respectively. The results for the Lax-Wendroff method are not very satisfactory, but for the Eulerian calculation additional damping can be added to the scheme to control the large oscillations. This does not work for the Lagrangian computation.

The FCT calculations are shown in figures 14 and 15. Figure 15 gives the results of the third order FCT method using Boris and Book's (ref. 11) version of the Lagrangian code. This code keeps the cartesian coordinates as the independent variables. The FCT results are much better than the Lax-Wendroff results. The third order FCT is slightly better than the Shasta FCT except for the terracing of the expansion wave. This is because Boris' formulation does not compute the x_a, x_b, y_a, y_b explicitly as in the present method.

The second problem solved was a two-dimensional reflection of an incident shock wave off a straight wall. The initial conditions and geometry are presented in figure 16. The incident shock wave is generated by the 1:5 wedge placed along the bottom wall of a straight channel. This shock wave reflects off the top wall as shown. The flow properties are chosen so that the reflection is regular and so that the flow is supersonic throughout thus the boundary computation of the present method can be compared with Abbett's scheme (ref. 9). Abbett's scheme is valid only for steady supersonic flow, so only the steady state results are shown. Another reason for choosing supersonic flow is that then the outflow conditions do not influence the upstream flow field.

The initial condition for computation is simply a straight channel with a Mach number 2.2 flow throughout. At $t = 0^+$ the bottom wall aft of $x = 1$ rotates upward about $x = 1$ until the final ramp angle of $\tan^{-1}(1/5)$ is reached. The computation proceeds until all the transients are washed downstream, which at this Mach number required a particle travel of approximately 2.2 ramp lengths, after the final ramp angle was attained. In physical time the ramp growth required 1 sec and the steady state was reached in another second. The total CPU time on a CDC 7600 for convergence was 135 sec, and the total number of time steps amounted to 300.

The results in terms of pressure profiles are shown in figures 17 and 18, for the Prandtl-Meyer (Abbett's scheme) and the normal momentum equation boundary correction. The oblique shock does not reach the foot of the ramp since a fairing function was fitted between $x = 0.9$ and 1.1 to eliminate the discontinuity in the surface slope and curvature at $x = 1$. The fairing function is a quintic polynomial whose value, slope, and curvature matches the prescribed boundary at the fairing positions.

The shocks are captured quite well, usually over three or four mesh points. The total number of mesh points is 51×21. It should be mentioned that the shocks cross the cells at an angle of approximately 45°, so there is no mesh alignment with the shock wave. The Prandtl-Meyer boundary correction gives slightly better results than the normal momentum correction; the latter has slight overshoots for the boundary streamlines. A comparison of the exact

solution with the computed results is shown in table 1. The incident shock angle is computed quite accurately; the reflected shock angle differs by 8-10%. This error in the Prandtl-Meyer boundary correction is caused by the violation of the isentropic condition as required by Abbett's scheme.

If the boundary method of Book, Boris and Hain (ref. 12), based on simple reflection principles, is followed for the above problem, no converged solution can be obtained. If the ramp angle was reduced to $\tan^{-1}(1/20)$ the results shown in figure 19 were obtained. Large overshoots appear in the streamlines near the boundary. The streamlines indicated by NY = 1 and NY = 15 are 1/2 cell from the surface. The surface pressures can be obtained by extrapolation. This is not done here since the results would be even worse than shown.

All of the two-dimensional results were obtained with the Shasta FCT algorithm. The third order FCT was not stable with the splitting procedure used in this report. The reason is not clear, but it seems that the coefficient of the fourth-order diffusion term of the modified equation, that is, $[(\Delta x^4/24\Delta t)\epsilon^2(\epsilon^2 - 1)]$ has the wrong sign (it is negative for $\epsilon^2 < 1$) for linear stability. It is conjectured that the nonlinear stability dominates the linear stability for the one-dimensional case but not for two-dimensional splitting procedures.

V. CONCLUDING REMARKS

A Lagrangian method has been developed to solve the unsteady inviscid gasdynamic equations by the FCT method. Unfortunately the boundary conditions as given by the original FCT method were not satisfactory and these were worked out for the special problems considered in this report. Shock waves and other flow discontinuities were captured accurately and monotonically.

The method works well, but only with the inclusion of the proper boundary conditions. The results are much better than those obtained by the mixed Euler-Lagrange methods of the Los Alamos group. The purely Lagrangian approach used here avoids the problem of mesh generation. However, we have avoided highly sheared flows so that the method did not require any mesh readjustment to maintain stability and accuracy, which can be a problem with Lagrangian methods.

APPENDIX A

DERIVATION OF GOVERNING EQUATIONS OF GAS DYNAMICS

FOR AN ARBITRARILY MOVING COORDINATE SYSTEM

We start with the Euler Equations

$$\vec{U}_t + \vec{F}_x + \vec{G}_y = 0 \tag{A1}$$

with

$$\vec{U} = \begin{bmatrix} \rho \\ \rho u \\ \rho v \\ \rho E \end{bmatrix} \quad ; \quad \vec{F} = \begin{bmatrix} \rho u \\ \rho u^2 + p \\ \rho uv \\ (\rho E + p)u \end{bmatrix} \quad ; \quad \text{and } \vec{G} = \begin{bmatrix} \rho v \\ \rho uv \\ \rho v^2 + p \\ (\rho E + p)v \end{bmatrix}$$

where

$$p = (\gamma - 1)\,\rho\left(E - \frac{u^2 + v^2}{2}\right)$$

We now want to transform to another arbitrarily moving coordinate system, call it (a, b, τ) where

$$\left.\begin{aligned} a &= a(x, y, t) \\ b &= b(x, y, t) \\ \tau &= t \end{aligned}\right\} \tag{A2}$$

and

$$\frac{1}{D} = \frac{\partial(x, y)}{\partial(a, b)} \equiv J$$

is the Jacobian of the transformation (a, b, τ) to (x, y, t).

Viviand's transformation technique (ref. 14) for a conservative system of equations applies and results in

$$\frac{\partial}{\partial\tau}(J\vec{U}) + \frac{\partial}{\partial a}\left(J\vec{U}\frac{\partial a}{\partial t} + \frac{\partial a}{\partial x}J\vec{F} + \frac{\partial a}{\partial y}J\vec{G}\right) + \frac{\partial}{\partial b}\left(J\vec{U}\frac{\partial b}{\partial t} + \frac{\partial b}{\partial x}J\vec{F} + \frac{\partial b}{\partial y}J\vec{G}\right) = 0 \tag{A3}$$

Since we have $a = a(x, y, t)$ and $b = b(x, y, t)$

$$\frac{da}{dt} = \frac{\partial a}{\partial x}\frac{\partial x}{\partial t} + \frac{\partial a}{\partial y}\frac{\partial y}{\partial t} + \frac{\partial a}{\partial t} = 0$$

where we require that a, b, t be independent variables.

Setting $\partial x/\partial t = u_m$ and $\partial y/\partial t = v_m$, i.e., the coordinate mesh velocity, we obtain

$$\frac{\partial a}{\partial t} = -u_m a_x - v_m a_y$$

and, similarly,

$$\frac{\partial b}{\partial t} = -u_m b_x - v_m b_y$$

Substituting into equation (A3) and simplifying,

$$\frac{\partial}{\partial \tau}(J\vec{U}) + \frac{\partial}{\partial a}\left[Ja_x(\vec{F} - u_m\vec{U}) + Jay(\vec{G} - v_m\vec{U})\right] + \frac{\partial}{\partial b}\left[Jb_x(\vec{F} - u_m\vec{U}) + Jby(\vec{G} - v_m\vec{U})\right] = 0 \quad \text{(A4)}$$

Now we need to invert the partial derivatives a_x, a_y, b_x, and b_y,

$$a_x = \frac{y_b}{J} \; ; \qquad b_x = \frac{-y_a}{J}$$

$$a_y = \frac{-x_b}{J} \; ; \quad \text{and} \qquad b_y = \frac{x_a}{J}$$

and setting $\tau = t$ results in

$$\frac{\partial}{\partial t}(J\vec{U}) + \frac{\partial}{\partial a}\left[J\vec{U}(u - u_m)\frac{y_b}{J} - J\vec{U}(v - v_m)\frac{x_b}{J} + \vec{C}\right] + \frac{\partial}{\partial b}\left\{-(J\vec{U})(u - u_m)\frac{y_a}{J} + J\vec{U}(v - v_m)\frac{x_a}{J} + \vec{D}\right\} = 0 \quad \text{(A5)}$$

where

$$J\vec{U} = \begin{bmatrix} J\rho \\ J\rho u \\ J\rho v \\ J\rho E \end{bmatrix} \; ; \qquad \vec{C} = \begin{bmatrix} 0 \\ y_b p \\ -x_b p \\ p(y_b u - x_b v) \end{bmatrix}$$

and

$$\vec{D} = \begin{bmatrix} 0 \\ -y_a p \\ x_a p \\ p(-y_a u + x_a v) \end{bmatrix}$$

System (A5) are the first four equations of system (1). The remaining six equations are the kinematic relations describing the mesh velocities. We have previously defined

$$\frac{\partial x}{\partial t} = u_m \quad \text{and} \quad \frac{\partial y}{\partial t} = v_m$$

Differentiating these two with respect to a and b obtains the last six equations of system (1).

APPENDIX B

THREE DIMENSIONAL LAGRANGIAN GASDYNAMICS EQUATIONS

The system of equations is

$$\vec{U} + \vec{F}_a + \vec{G}_b + \vec{H}_c + \vec{S} = 0 \qquad \text{(B1)}$$

with

$$\vec{U} = \begin{bmatrix} J\rho \\ J\rho u \\ J\rho v \\ J\rho w \\ J\rho E \\ x \\ y \\ z \end{bmatrix}; \quad \vec{F} = \begin{bmatrix} 0 \\ p(y_b z_c - y_c z_b) \\ p(x_c z_b - x_b z_c) \\ p(x_b y_c - x_c y_b) \\ pJu^M \\ 0 \\ 0 \\ 0 \end{bmatrix}$$

$$\vec{G} = \begin{bmatrix} 0 \\ p(y_c z_a - y_a z_c) \\ p(x_a z_c - x_c z_a) \\ p(x_c y_a - x_a y_c) \\ pJv^M \\ 0 \\ 0 \\ 0 \end{bmatrix}; \quad \vec{H} = \begin{bmatrix} 0 \\ p(y_a z_b - y_b z_a) \\ p(x_b z_a - x_a z_b) \\ p(x_a y_b - x_b y_a) \\ pJw^M \\ 0 \\ 0 \\ 0 \end{bmatrix}; \text{ and } \vec{S} = \begin{bmatrix} 0 \\ 0 \\ 0 \\ 0 \\ 0 \\ -u \\ -v \\ -w \end{bmatrix}$$

The nine other kinematic relations obtained by differentiating the last three equations of system (B1) with respect to a, b, and c have not been included. They are required only to keep the system strongly conservative. The Jacobian of the transformation (a,b,c,t) to (x,y,z,t) is

$$J = \frac{\partial(x,y,z)}{\partial(a,b,c)}$$

$$= x_a\,(y_b z_c - y_c z_b) + y_b\,(x_a z_c - x_c z_a) + z_c\,(x_a y_b - x_b y_a)$$

The superscript M again refers to the velocity components in the moving coordinate system (a,b,c). Thus,

$$u^M = a_x u + a_z v + a_z w$$
$$v^M = b_x u + b_y v + b_z w$$
$$w^M = c_x u + c_y v + c_z w$$

where

$$a_x = \frac{1}{J}\left\{y_b z_c - y_c z_b\right\}$$
$$a_y = \frac{1}{J}\left\{x_c z_b - x_b z_c\right\}$$
$$a_z = \frac{1}{J}\left\{x_b y_c - x_c y_b\right\}$$
$$b_x = \frac{1}{J}\left\{y_c z_a - y_a z_c\right\}$$
$$b_y = \frac{1}{J}\left\{x_a z_c - x_c z_a\right\}$$
$$b_z = \frac{1}{J}\left\{x_c y_a - x_a y_c\right\}$$
$$c_x = \frac{1}{J}\left\{y_a z_b - y_b a_a\right\}$$
$$c_y = \frac{1}{J}\left\{x_b z_a - x_a z_b\right\}$$

and

$$c_z = \frac{1}{J}\left\{x_a y_b - x_b y_a\right\}$$

REFERENCES

1. Bailey, F. R.; and Ballhaus, W. F.: Aerodynamic Analyses Requiring Advanced Computers, Part II. NASA SP-347, 1975.

2. Boerstoel, J. W.: Symposium Transsonicum II, IUTAM Symposium, Goettingen, Springer-Verlag, Berlin, 1975.

3. Jameson, A.: Symposium Transsonicum II, IUTAM Symposium, Goettingen, Springer-Verlag, Berlin, 1975.

4. Rizzi, A.: Symposium Transsonicum II, IUTAM Symposium, Goettingen, Springer-Verlag, Berlin, 1975.

5. Thompson, J. F.; Thames, F. C.; and Mastin, C. W.: J. Comp. Physics 15, 1974, pp. 299-319.

6. Harlow, F. H.; and Amsden, A. A.: J. Comp. Physics 16, 1974, pp. 1-19.

7. Lamb, Horace: Hydrodynamics. Dover Republication, 1952.

8. Warming, R.; and Hyett, J.: J. Comp. Physics 14, No. 2, 1974.

9. Abbett, M. J.: Boundary Condition Calculation Procedures for Inviscid Supersonic Flow Fields. Proceedings AIAA Comp. Fluid Dynamic Conference. Palm Springs, California, July 19-20, 1973.

10. Lerat, A.; and Peyret, R.: Proceedings of the Fourth International Conference on Numerical Methods in Fluid Dynamics, Boulder, Colorado, 1974.

11. Boris, J. P.; and Book, D. L.: NRL Mem. Rep. 3237, 1976.

12. Book, D. L.; Boris, J. P.; and Hain, K.: NRL Mem. Rep. 3021, 1975.

13. Beam, R. M.; and Warming, R. F.: J. Comp. Physics 22, 1976, pp. 87-110.

14. Viviand, H.: La Recherche Aerospatiale, no. 1, 1974, pp. 65-66.

TABLE 1.- COMPARISON OF EXACT SOLUTION WITH THE PRANDTL-MEYER AND NORMAL MOMENTUM BOUNDARY CORRECTION FOR THE REGULAR SHOCK WAVE REFLECTION

	M_1	M_2	M_3	θ_1 (deg)	θ_2 (deg)
Exact	2.2	1.87	1.47	37.2	46.6
Prandtl-Meyer	2.2	1.8	1.42	37.2	50.3
Normal momentum	2.2	1.81	1.4	37.8	51.6

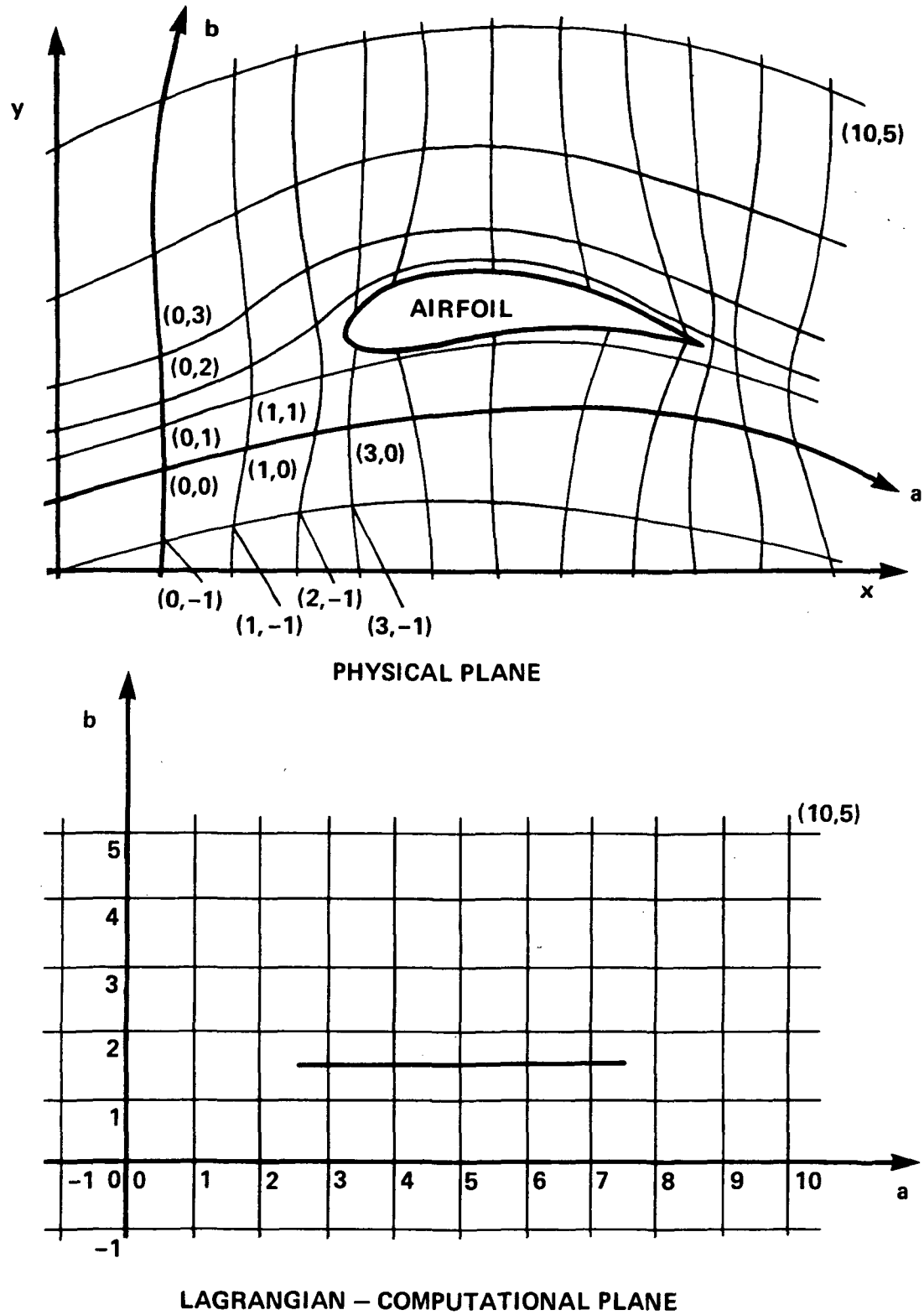

Figure 1.- Transformation of physical to computational plane.

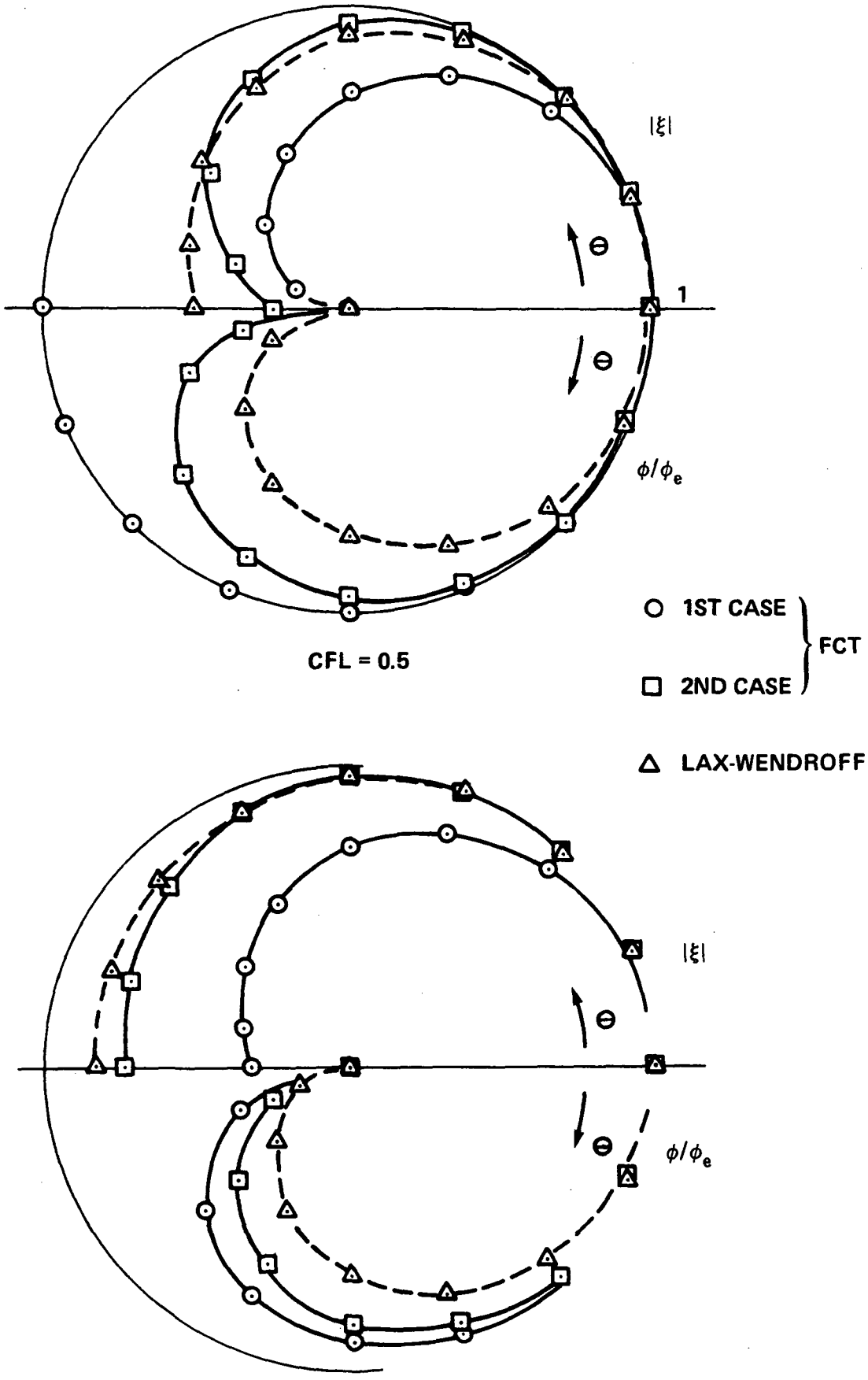

Figure 2.- Von Neumann stability properties for the Lax-Wendroff and SHASTA FCT method.

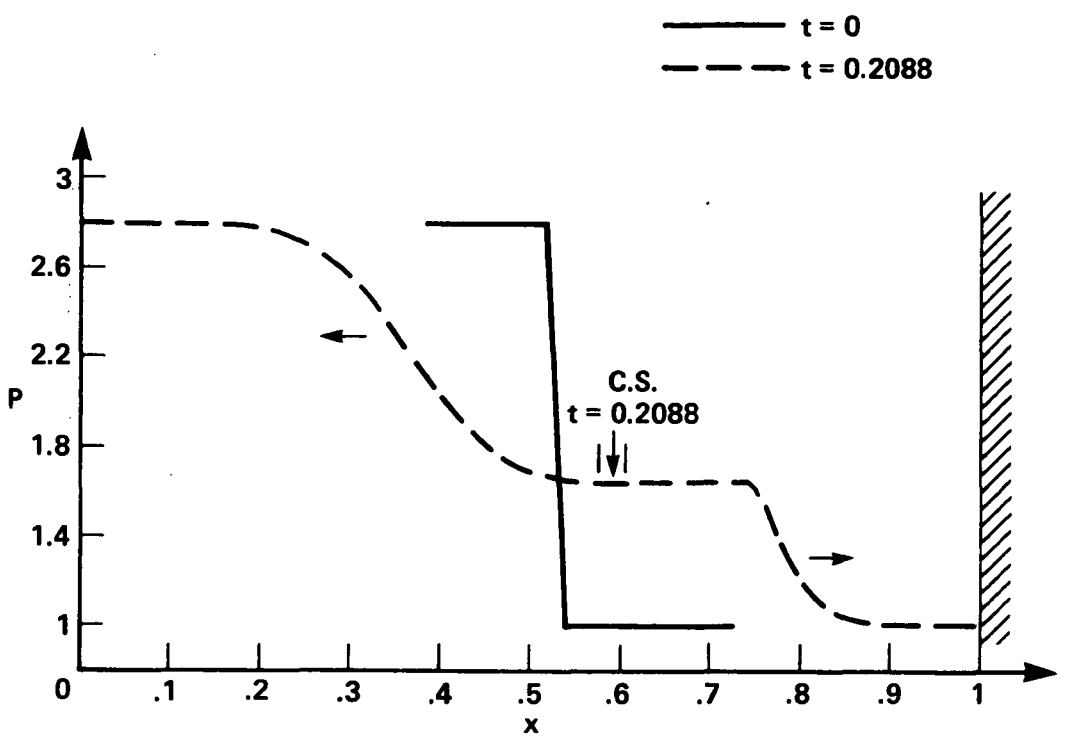

(a) Step 1 - Diffused transport solution, 51 points.

Figure 3.- Pressure profiles in the Lagrangian formulation solved by the FCT method.

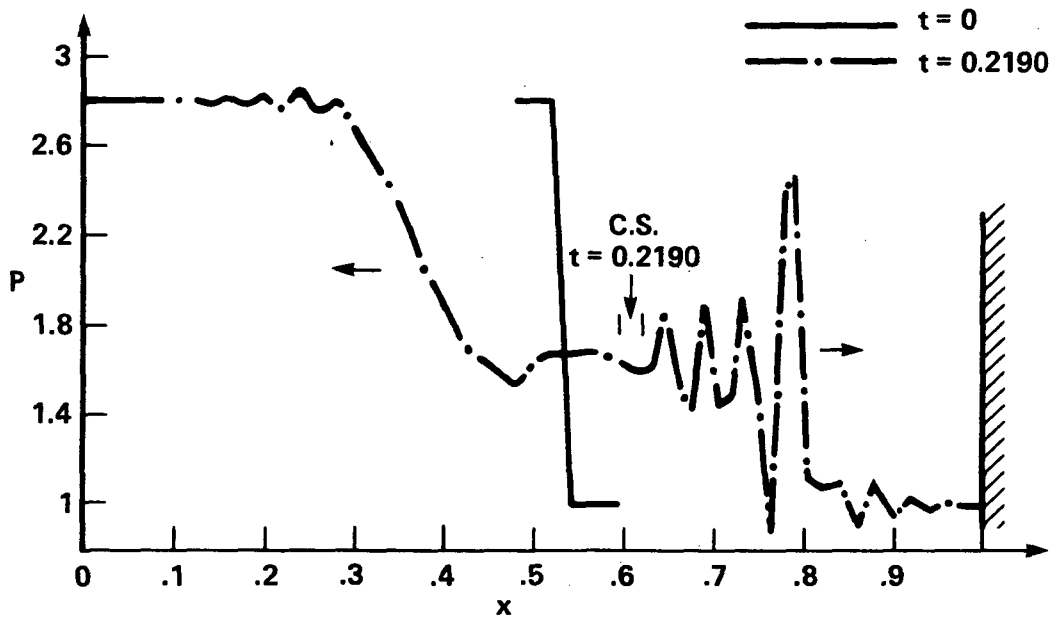

(b) Step 2 - Antidiffused solution with no flux limiter.

Figure 3.- Continued.

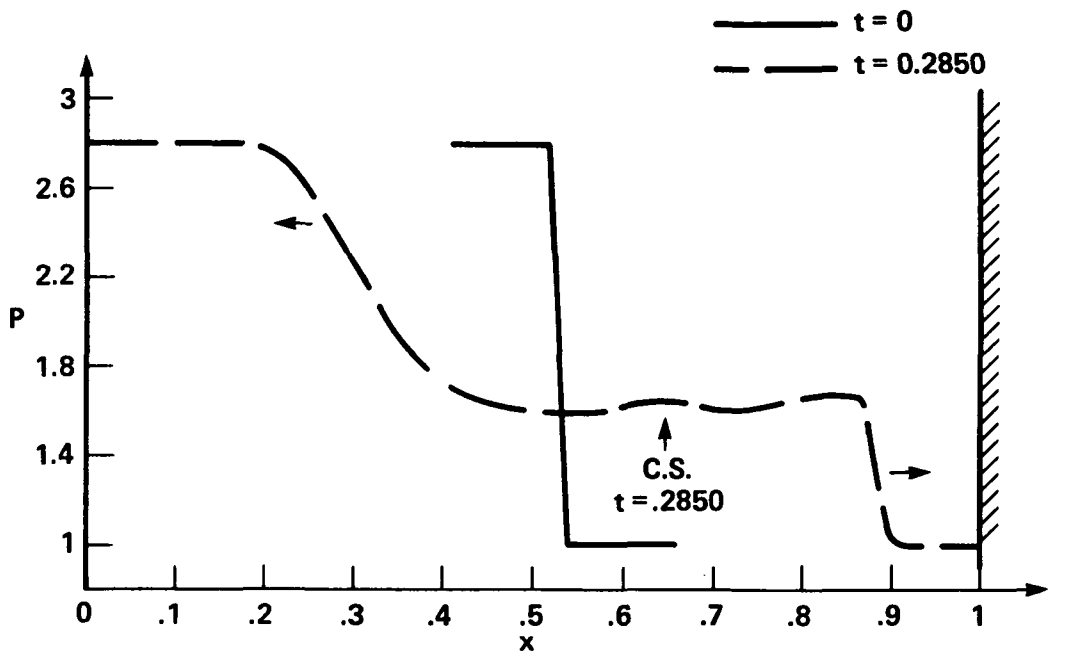

(c) Step 3 - Flux-limited antidiffused solution.

Figure 3.- Concluded.

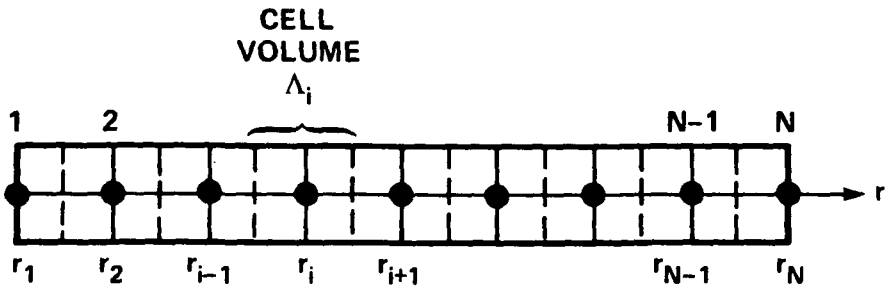

Figure 4.- Rectangular network of the third-order FCT algorithm.

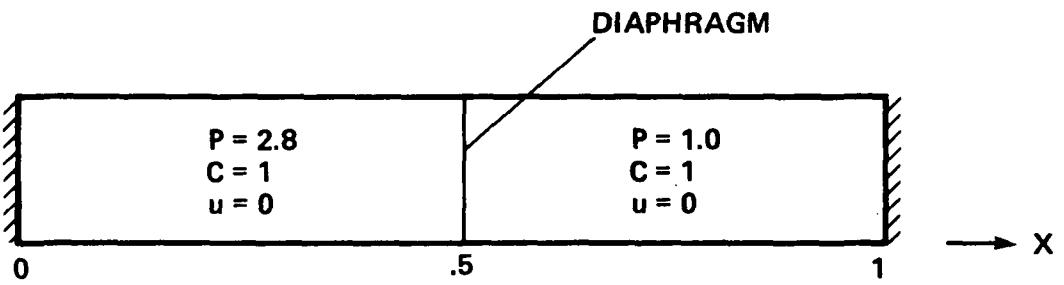

Figure 5.- The one-dimensional Riemann problem.

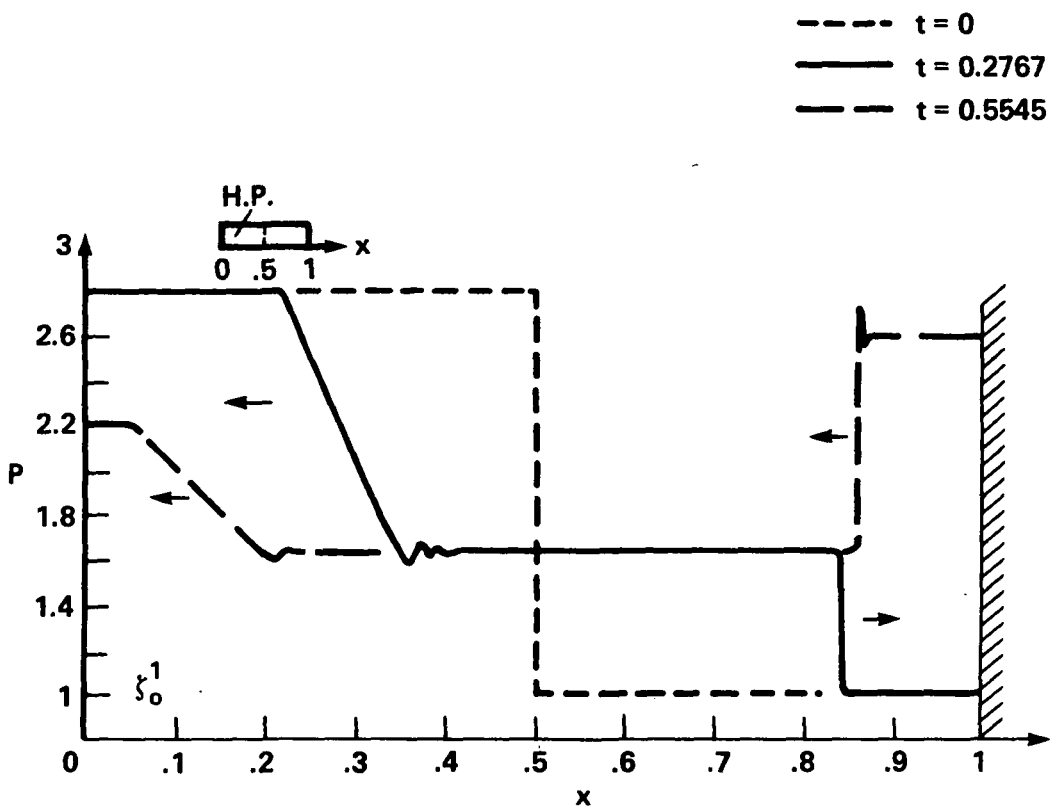

'igure 6.- Riemann problem, Eulerian coordinates, solved numerically with the MacCormack scheme. Pressure as a function of x and time t, 500 points, CFL = 1.0, and reflecting boundaries.

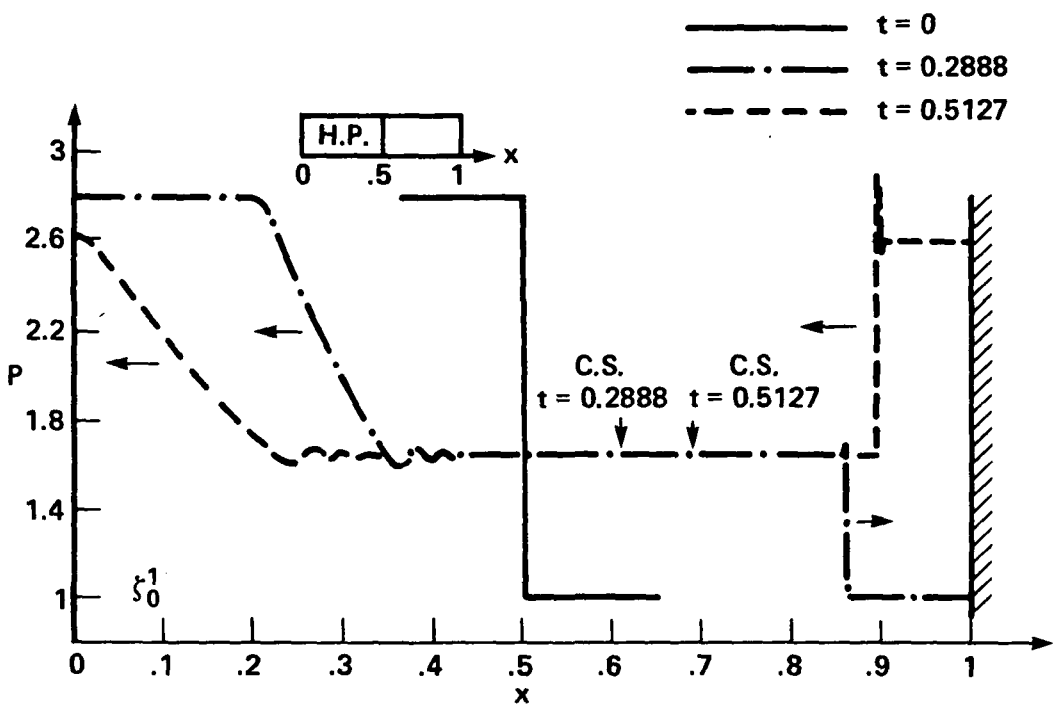

(a) Pressure as a function of x and t. Nonequal masses in the fluid cells, 500 points, CFL = 0.9, and reflecting boundaries.

Figure 7.- Riemann problem, Lagrangian coordinates, solved with MacCormack's scheme.

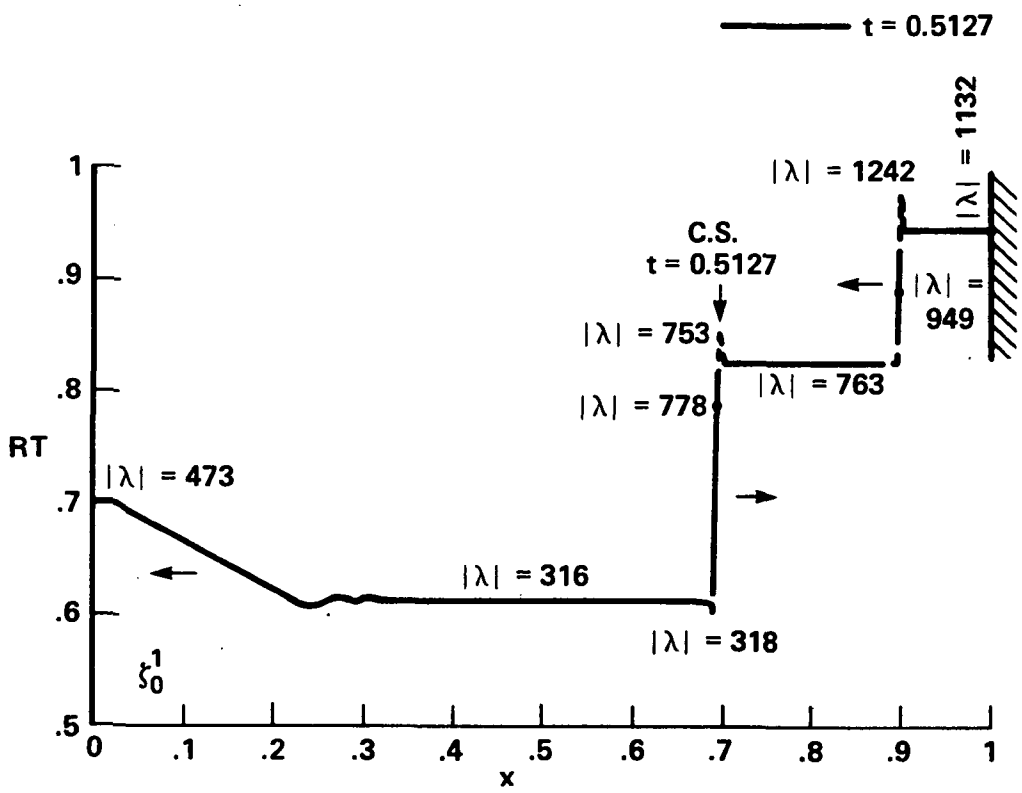

(b) Temperature as a function of x at time t = 0.5127. Nonequal masses in the fluid cells, 500 points, CFL = 0.9, and reflecting boundaries.

Figure 7.- Concluded.

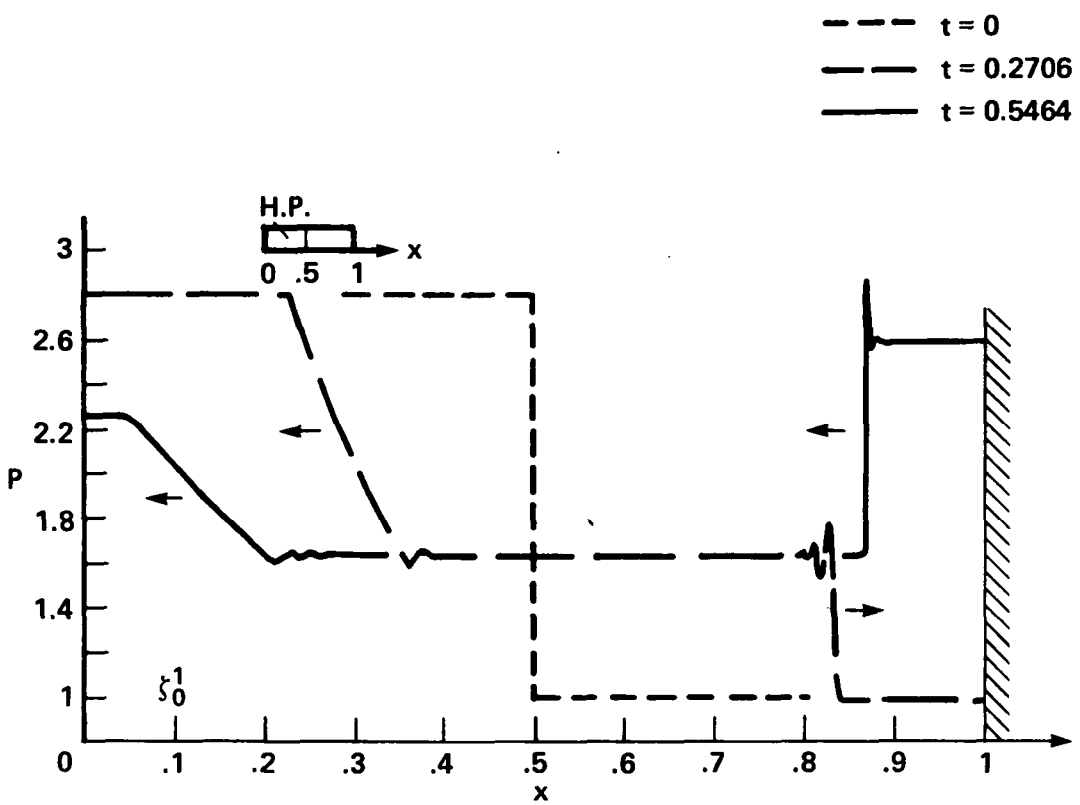

Figure 8.- Riemann problem, Lagrangian coordinates, solved with MaCormack's scheme. Pressure as a function of x and t. Equal masses in the fluid cells, 500 points, CFL = 1.0, and reflecting boundaries.

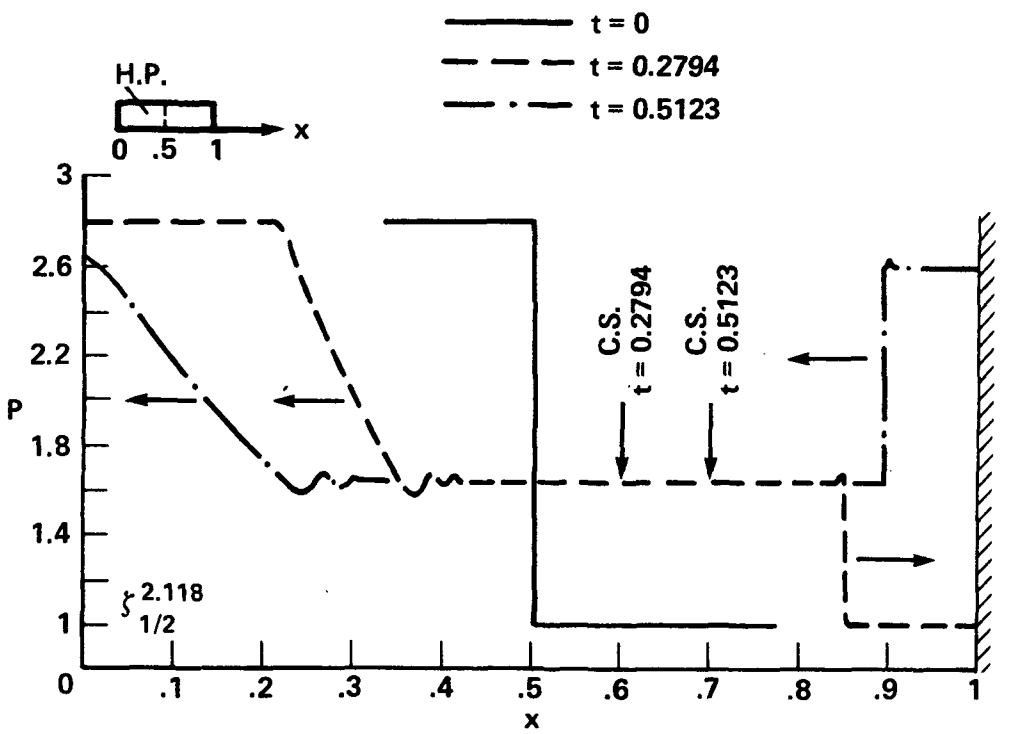

Figure 9.- Riemann problem, Lagrangian coordinates, solved with the generalized Lax-Wendroff scheme. Pressure as a function of x and t. Nonequal masses in the fluid cells, 500 points, CFL = 0.9, and reflecting boundaries.

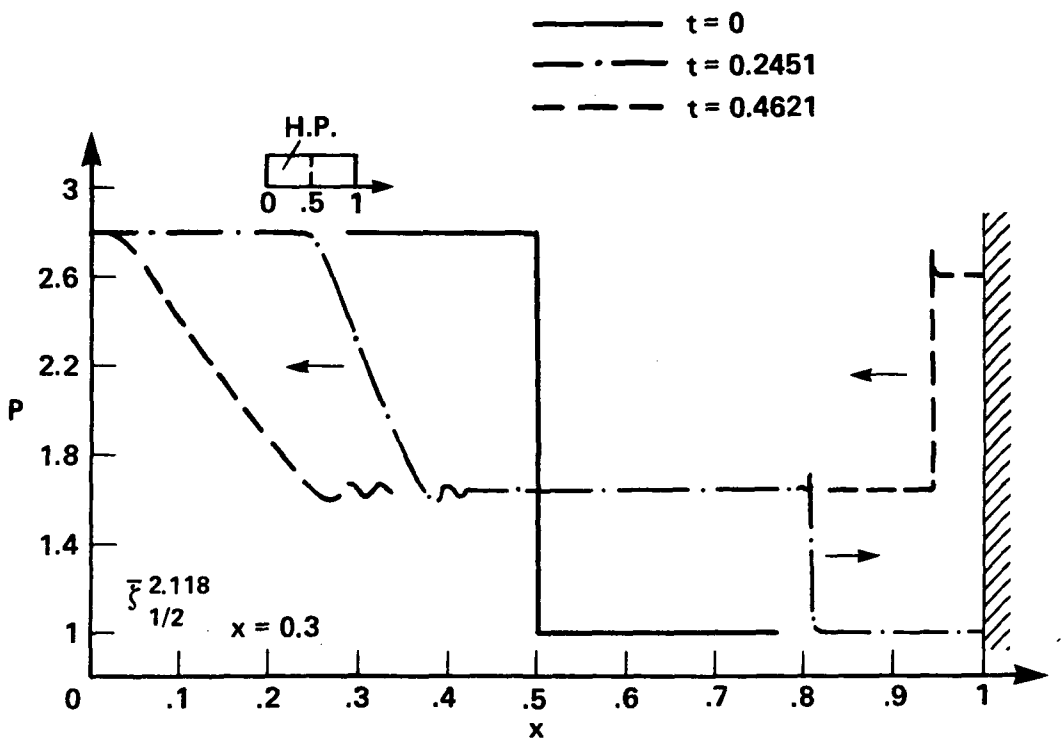

Figure 10.- Riemann problem, Lagrangian coordinates, solved with the generalized Lax-Wendroff scheme with artificial dissipation. Pressure as a function of x and t. Nonequal masses in the fluid cells, 500 points, and reflecting boundaries.

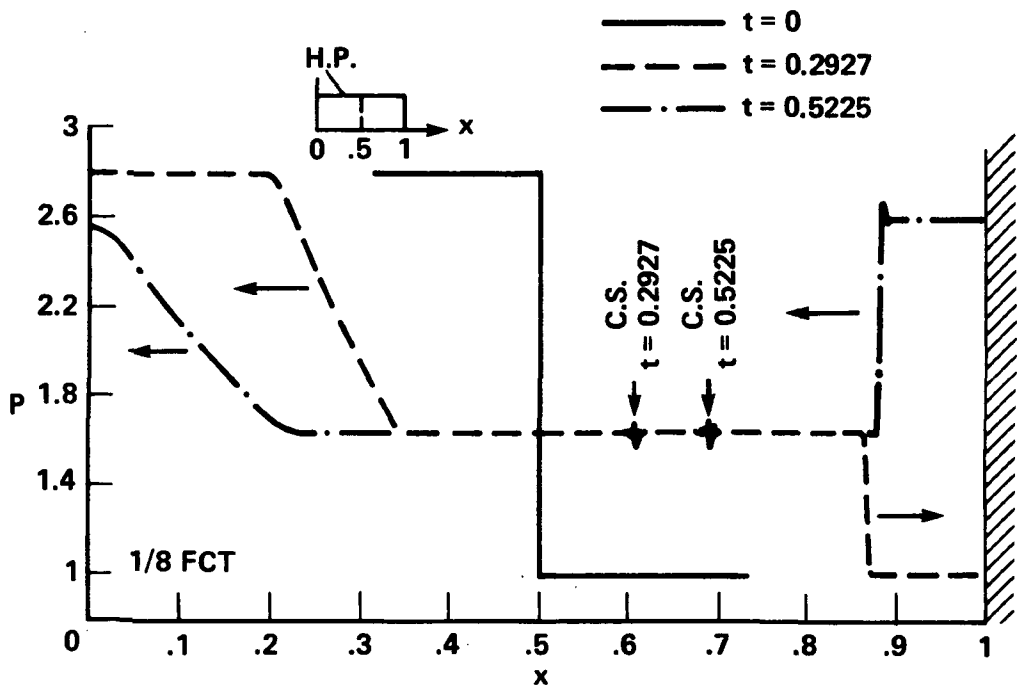

Figure 11.- Riemann problem, Lagrangian coordinates, solved with the 1/8 FCT scheme. Pressure as a function of x and t. Nonequal masses in the fluid cells, 500 points, and reflecting boundaries.

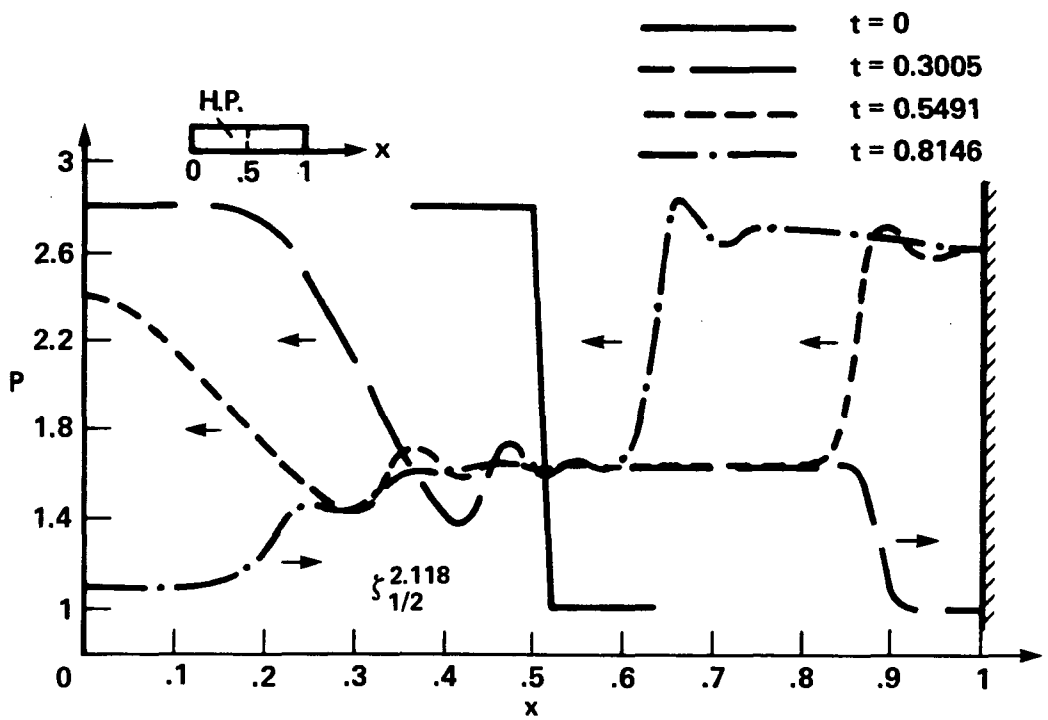

Figure 12.- Riemann problem, Eulerian coordinates, solved by the optimum generalized Lax-Wendroff scheme. Pressure as a function of x and t. Nonequal masses in the fluid cells, 51 points, and three-point boundary reflection.

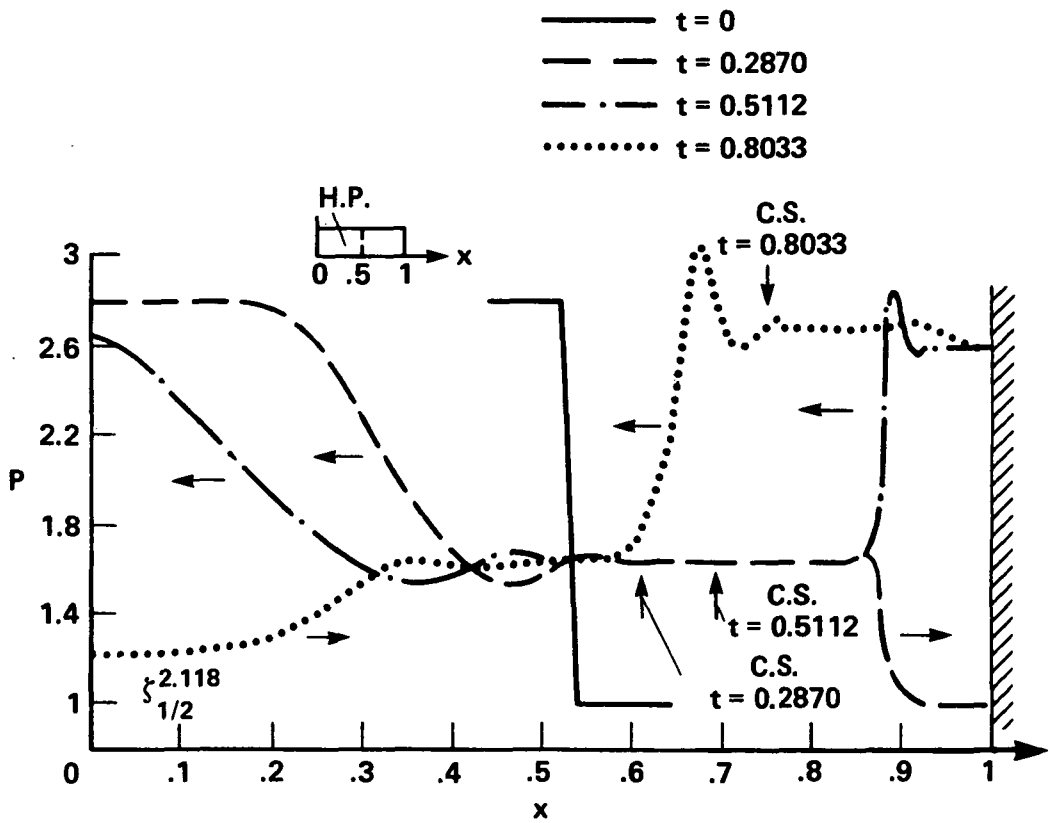

Figure 13.- Riemann problem, Lagrangian coordinates, solved by the optimum generalized Lax-Wendroff scheme. Pressure as a function of x and t. Nonequal masses in the fluid cells, 51 points, and reflecting boundaries.

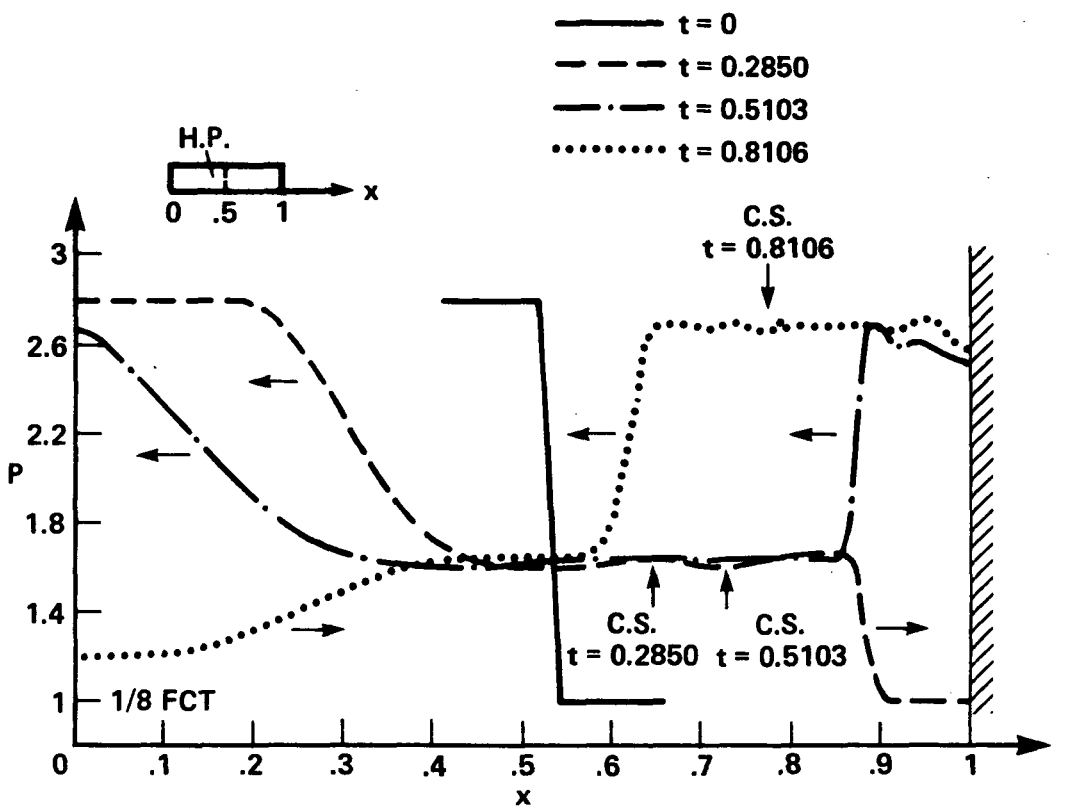

Figure 14.- Riemann problem, Lagrangian coordinates, solved by the SHASTA 1/8 FCT scheme. Pressure as a function of x and t. Nonequal masses in the fluid cells, 51 points, and reflecting boundaries.

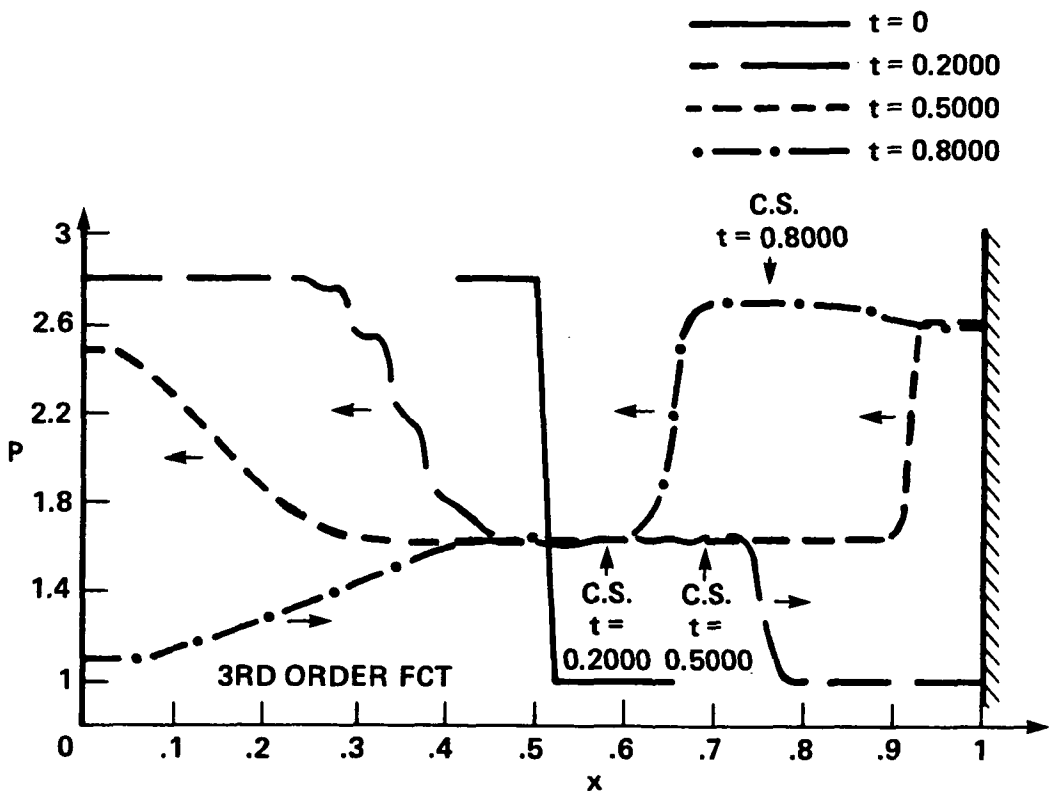

Figure 15.- Riemann problem, Lagrangian coordinates (Boris' version - March 1976), solved by the third order FCT scheme. Pressure as a function of x and t. Nonequal masses in the fluid cells, 50 points, and reflecting boundaries.

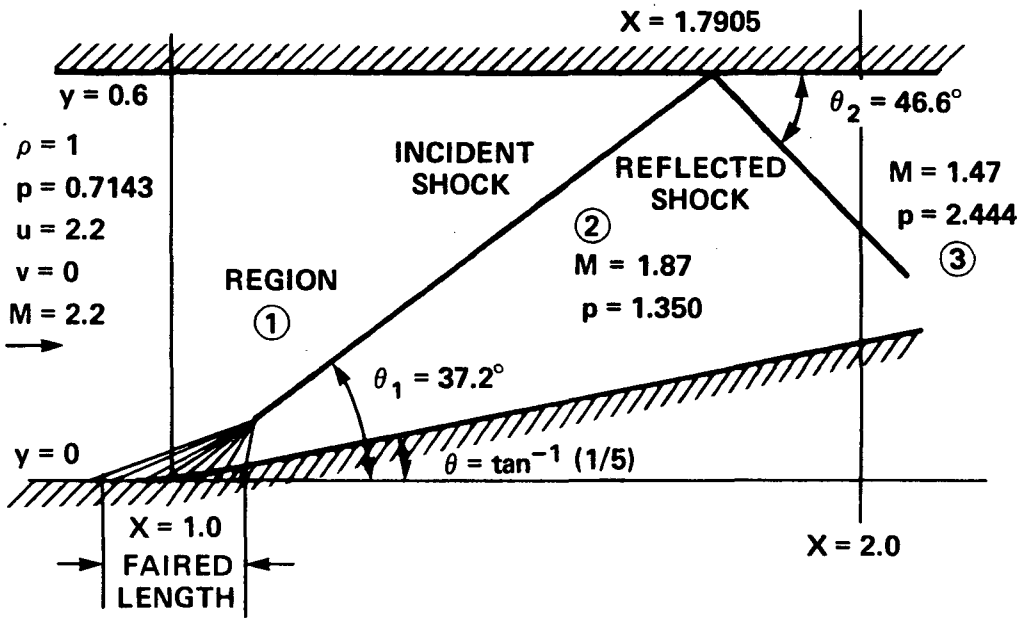

Figure 16.- Regular oblique shock-wave reflection pattern - exact solution.

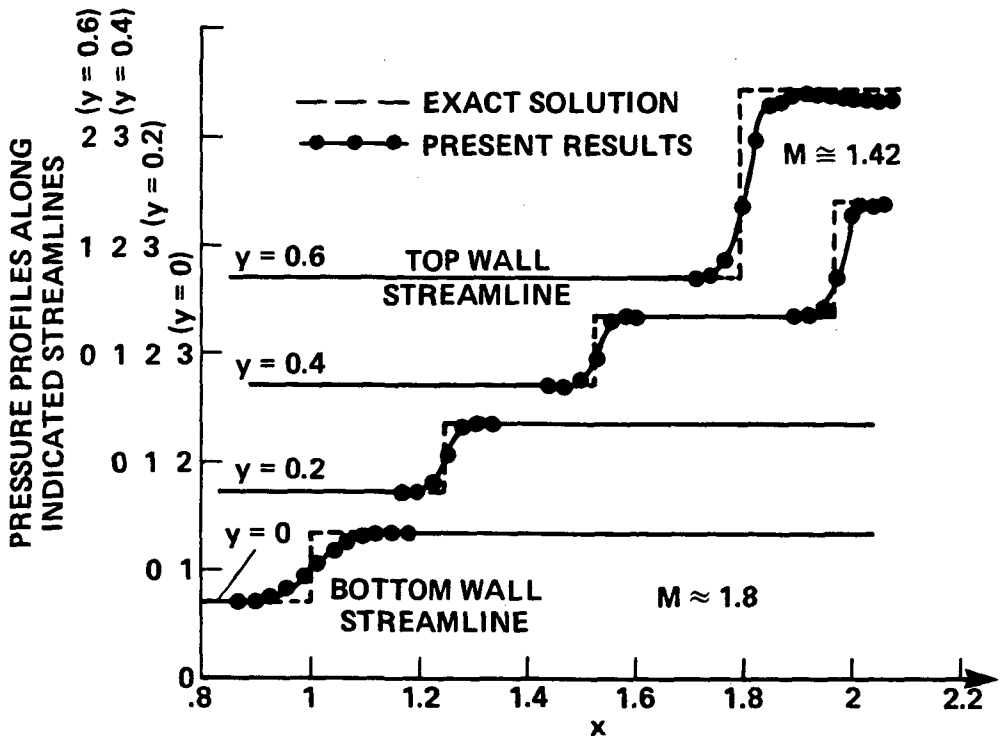

Figure 17.- Regular oblique shock-wave relection. Prandtl-Meyer boundary correction, 1/5 ramp, Mach no. = 2.2.

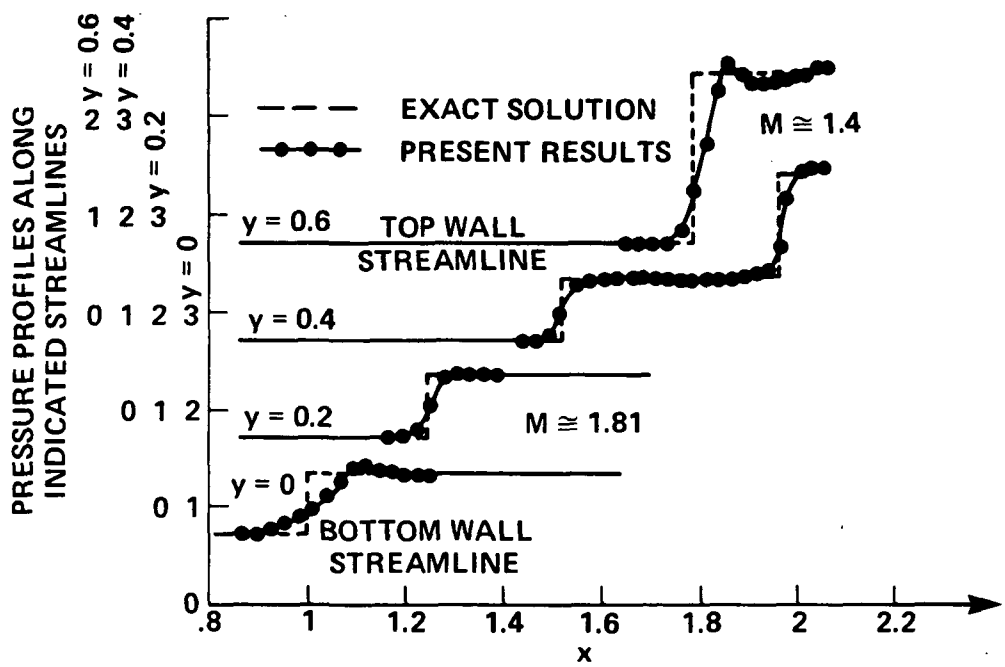

Figure 18.- Regular oblique shock-wave reflection. Normal momentum boundary correction, 1/5 ramp, Mach no. = 2.2.

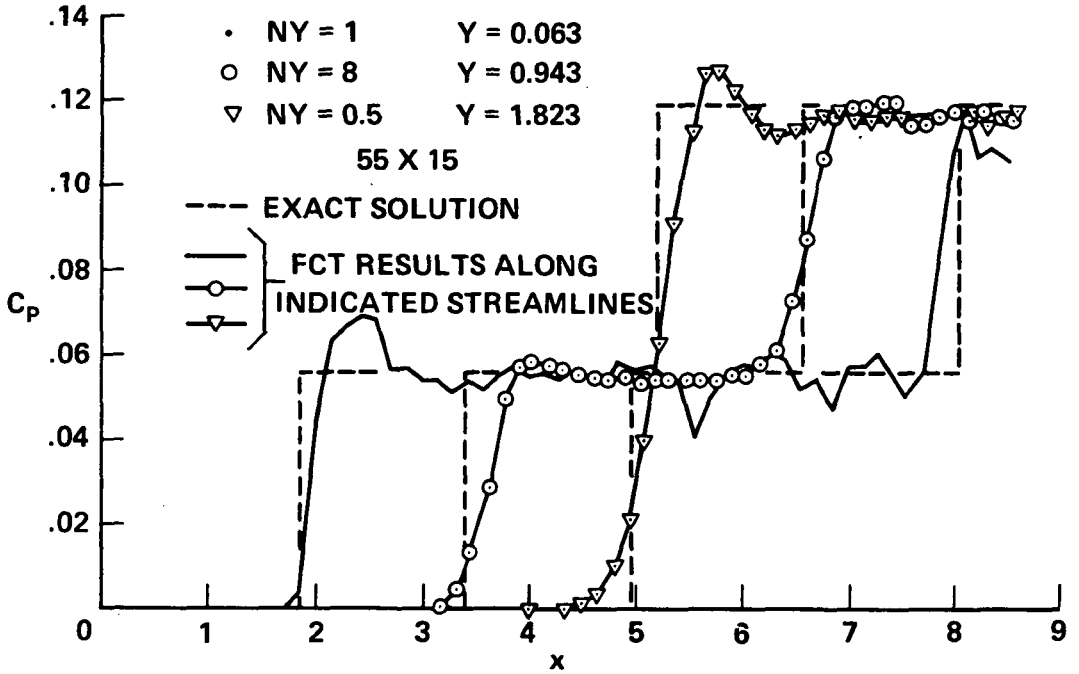

Figure 19.- Regular oblique shock-wave reflection. Boundary conditions computed by Boris' procedure (1975), 1/20 ramp, Mach no. = 2.2.

1. Report No.	2. Government Accession No.	3. Recipient's Catalog No.
NASA TM-78456		

4. Title and Subtitle	5. Report Date
LAGRANGIAN COMPUTATION OF INVISCID COMPRESSIBLE FLOWS	6. Performing Organization Code

7. Author(s)	8. Performing Organization Report No.
G. H. Klopfer*	A-7288

9. Performing Organization Name and Address	10. Work Unit No.
NASA Ames Research Center Moffett Field, California 94035	505-06-11-05-00
	11. Contract or Grant No.

12. Sponsoring Agency Name and Address	13. Type of Report and Period Covered
National Aeronautics and Space Administration Washington, D. C. 20546	Technical Memorandum
	14. Sponsoring Agency Code

15. Supplementary Notes

*NRC Resident Research Associate

16. Abstract

A Lagrangian method is developed to solve the Euler equations of gas dynamics. The solution of the equations is obtained by a numerical computation with the well-known Flux-Corrected-Transport (FCT) numerical method. This procedure is modified so that the boundary treatment is accurate and relatively simple. Shock waves and other flow discontinuities are captured monotonically without any type of fitting procedures. The Lagrangian method is employed so that the problem of mesh generation is completely avoided. The method is applicable to all Mach numbers except the low subsonic range where compressibility effects are small. The method is applied to a one-dimensional Riemann problem (shock tube) and to a two-dimensional supersonic channel flow with reflecting shock waves.

17. Key Words (Suggested by Author(s))	18. Distribution Statement
Compressible flows Lagrangian methods Numerical methods	Unclassified STAR Category - 64

19. Security Classif. (of this report)	20. Security Classif. (of this page)	21. No. of Pages	22. Price*
Unclassified	Unclassified	59	$4.50

*For sale by the National Technical Information Service, Springfield, Virginia 22161